The Abdus Salam
International Centre for Theoretical Physics

United Nations
Educational, Scientific
and Cultural Organization

International Atomic
Energy Agency

World Year of PHYSICS 2005

SMR.1664 - 2

Conference on Single Molecule Magnets and Hybrid Magnetic Nanostructures

27 June - 1 July 2005

Molecular Magnets
Spectroscopic and Dynamic Studies

Martin DRESSEL
1. Physikalisches Institut
Universitat Stuttgart
Pfaffenwaldring 57
D-70550 Stuttgart
GERMANY

These are preliminary lecture notes, intended only for distribution to participants

Molecular Magnets

Spectroscopic and Dynamic Studies

Martin Dressel

1. Physikalisches Institut, Universität Stuttgart

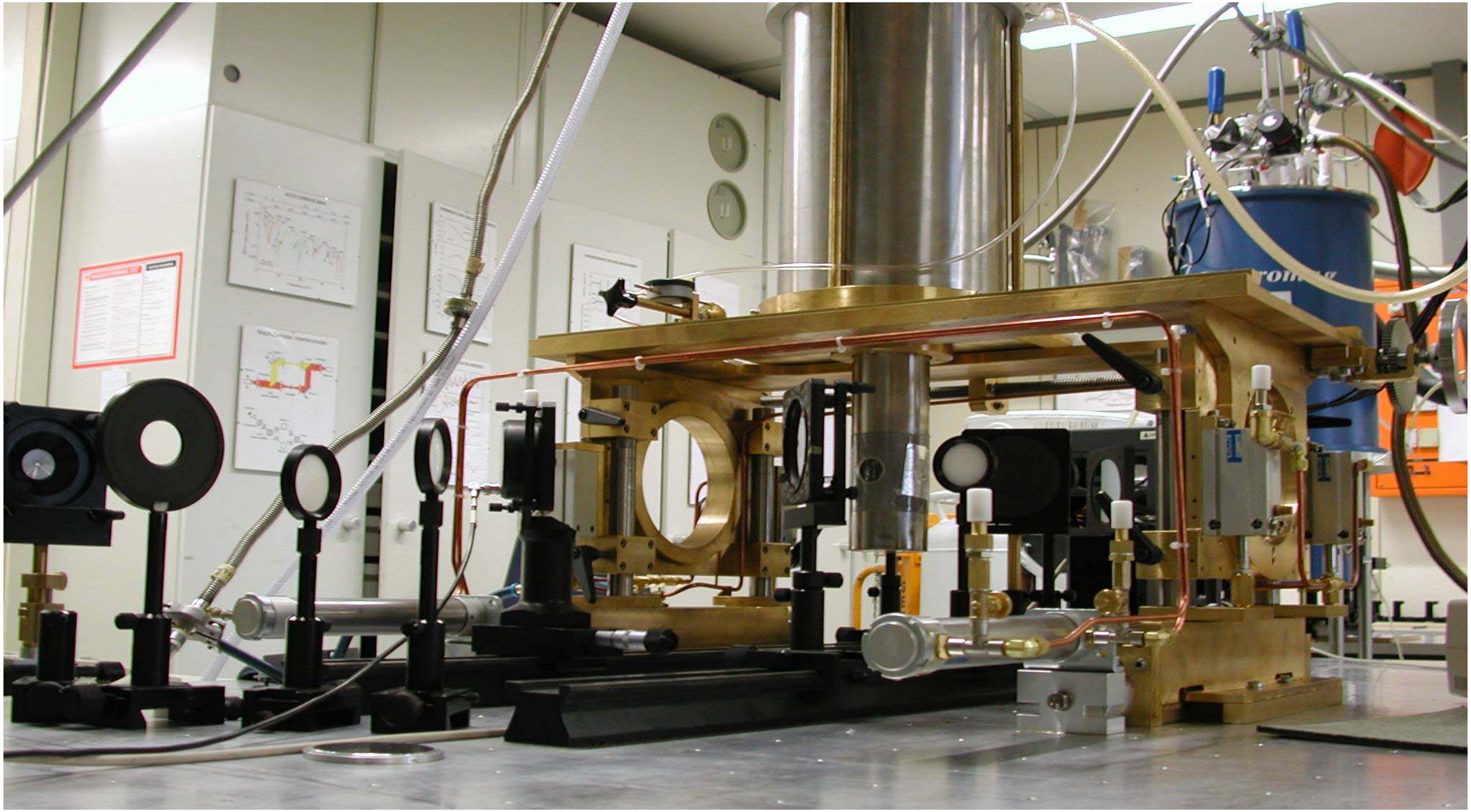

Molecular Magnets

Spectroscopic and Dynamic Studies

Martin Dressel
1. Physikalisches Institut, Universität Stuttgart

Outline

1. **Introduction**
   molecular magnets: $Mn_{12}ac$
2. **Frequency-Domain Magnetic Resonance Spectroscopy**
   parameters of Hamiltonian, lineshape
3. **Geometrical and Polarization Dependence**
   Voigt *vs.* Faraday configuration
   zero-field cooled *vs.* field cooled
4. **Magnetic Quantum Tunneling**
   relaxation, tunneling
   magnetic hole burning

Universität Stuttgart
J. van Slageren, B. Gorshunov,
S. Vongtragool, N. Kirchner

Russian Academy of Sciences, Moscow
A.A. Mukhin

Università di Firenze
D. Gatteschi, A. Caneschi

Universitat de Barcelona
J. Tejada

Molecular Magnet

$Mn_{12}ac$

$[Mn_{12}O_{12}(CH_3COO)_{16}(H_2O)_4]\cdot 2CH_3COOH\cdot 4H_2O$

single crystal with tetragonal symmetry S_4
a = 1.732 nm   b = 1.239 nm
unit cell volume 3716 Å^3

mixed valence cluster with 8 Mn^{3+} and 4 Mn^{4+}

ferrimagnetic cluster with ground state of **S = 10**

uniaxial magnetic anisotropy due to the crystal field

$H = DS_z^2$

barrier height:

$E = DS^2/k_B = 65$ K

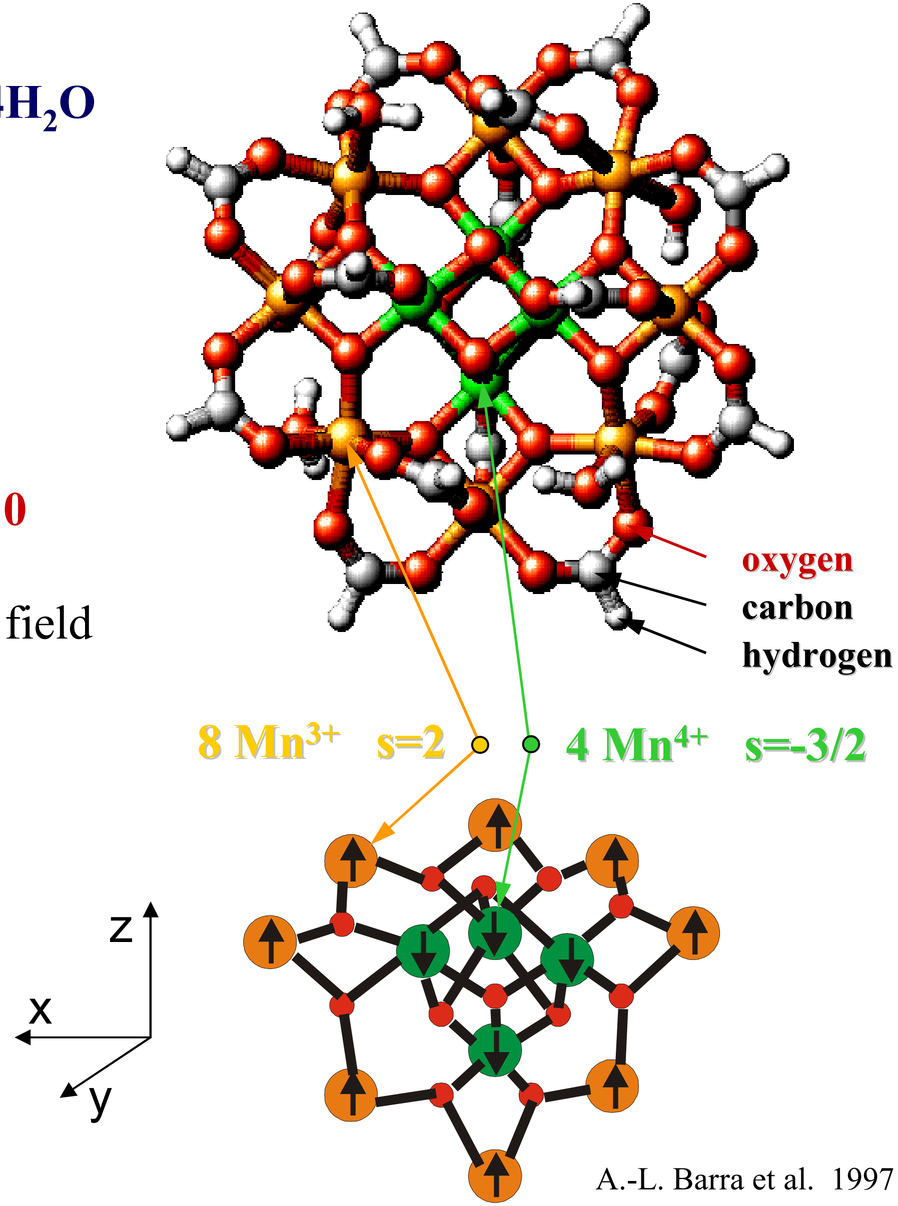

A.-L. Barra et al. 1997

Spectroscopy on Molecular Magnets

energy levels

Spin Hamiltonian of $Mn_{12}ac$

$H = DS_z^2$

base $|S^2, m\rangle$ with $m = -S, -(S+1), \ldots, S$

$2S+1$ energy levels

matrix element $\langle S^2, m \,|\, H \,|\, S^2, n \rangle$

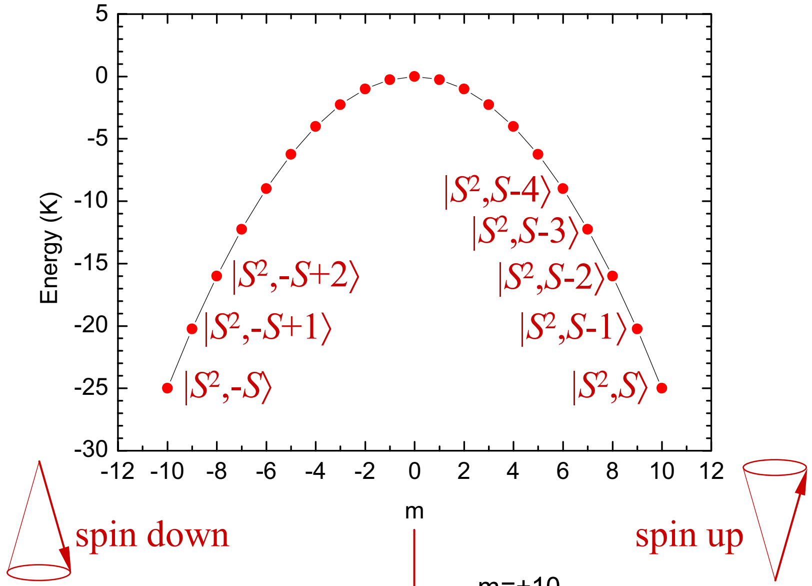

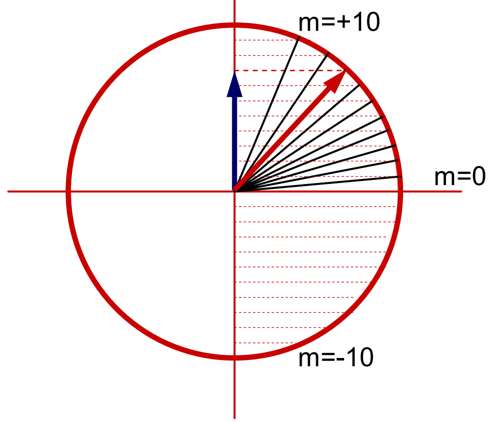

The splitting of the energy levels is of the order of

1 – 50 K **0.7 – 40 cm^{-1}** **30 – 1400 GHz**

⇒high-frequency ESR

determines **the parameters of the Hamiltonian**
the low-energy excitations
internal fields, disorder, environment

High-Frequency ESR Spectrometer

30 GHz - 1500 GHz , 1 cm^{-1} – 50 cm^{-1}

sources: backward wave oscillators
monochromatic, coherent, polarized
continuous, tunable, powerful

lenses: polyethylene, teflon

beamsplitter, polarizer:
free standing wire grids

phase shifter:
mirror and wire grid

detector: Golay cell,
He-cooled bolometer

cryostat: 0.4 K – 300 K

magnet: 0 – 8 Tesla
split ring, superconducting
Voigt, Faraday geometry

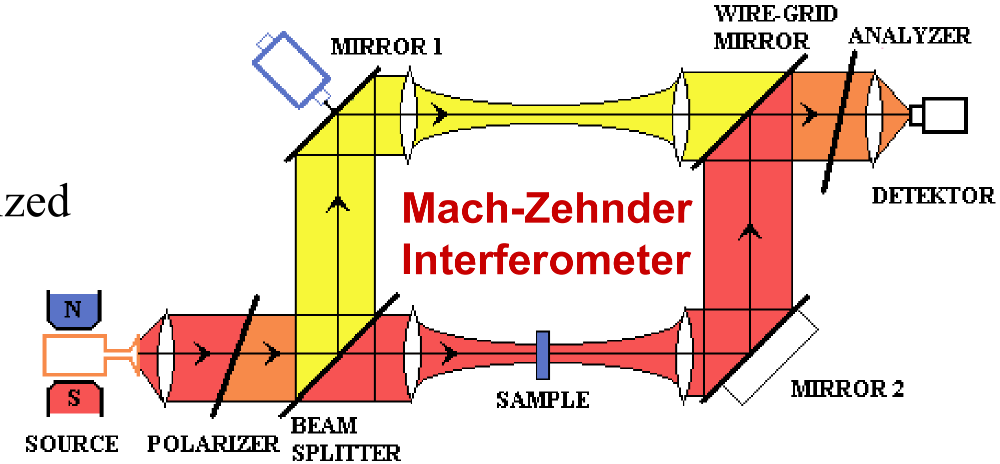

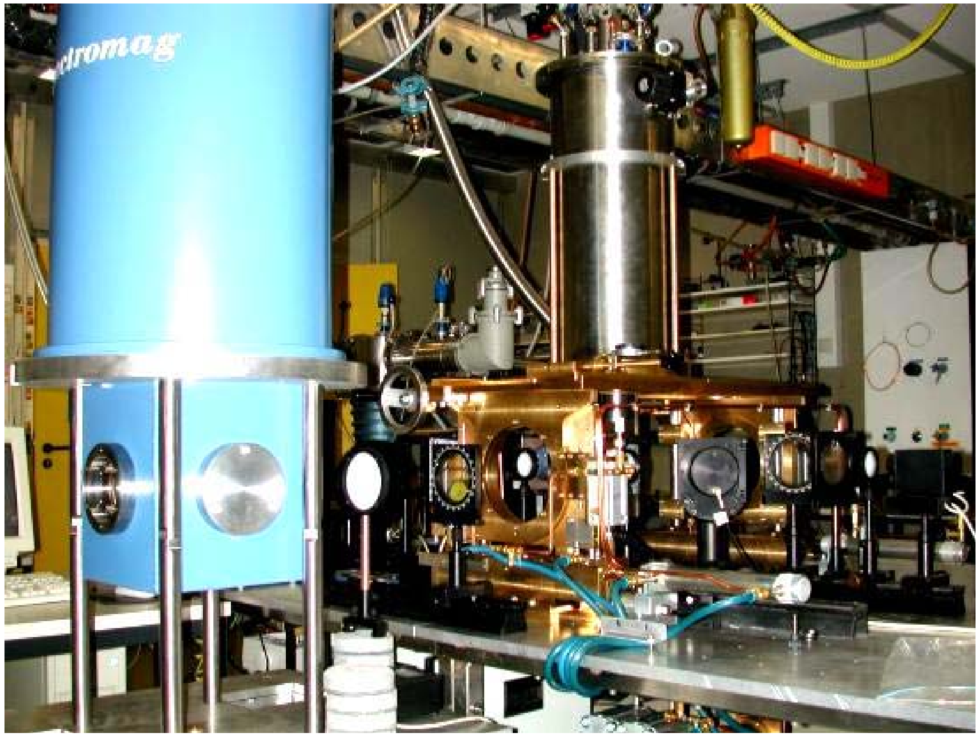

Radiation Sources

backward wave oscillators

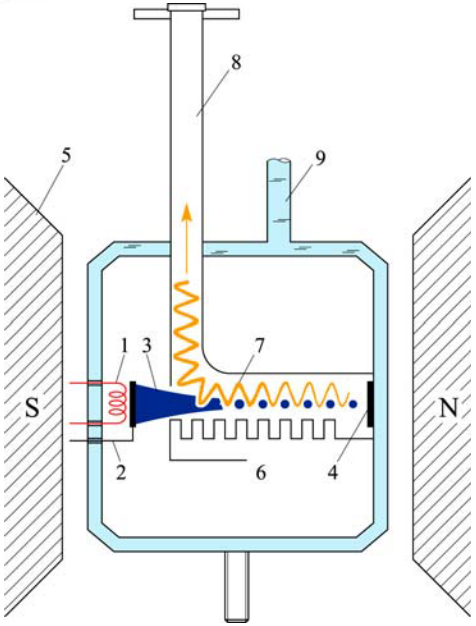

Output power spectra of BWOs

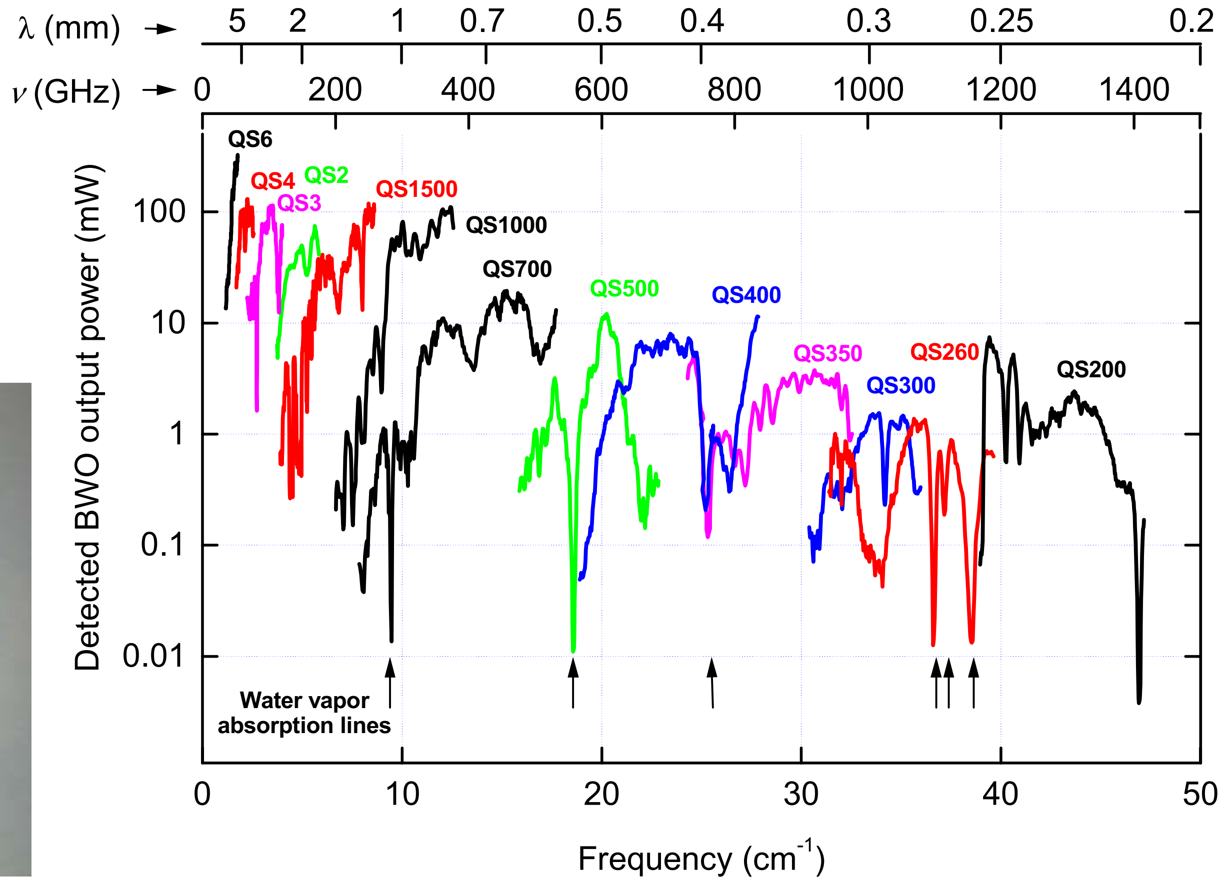

Radiation Sources

backward wave oscillators

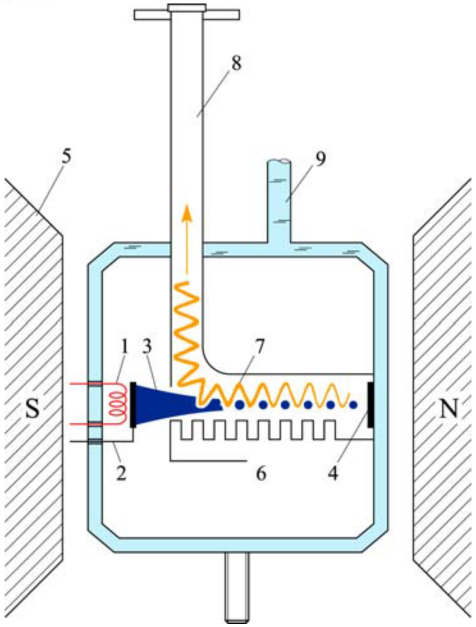

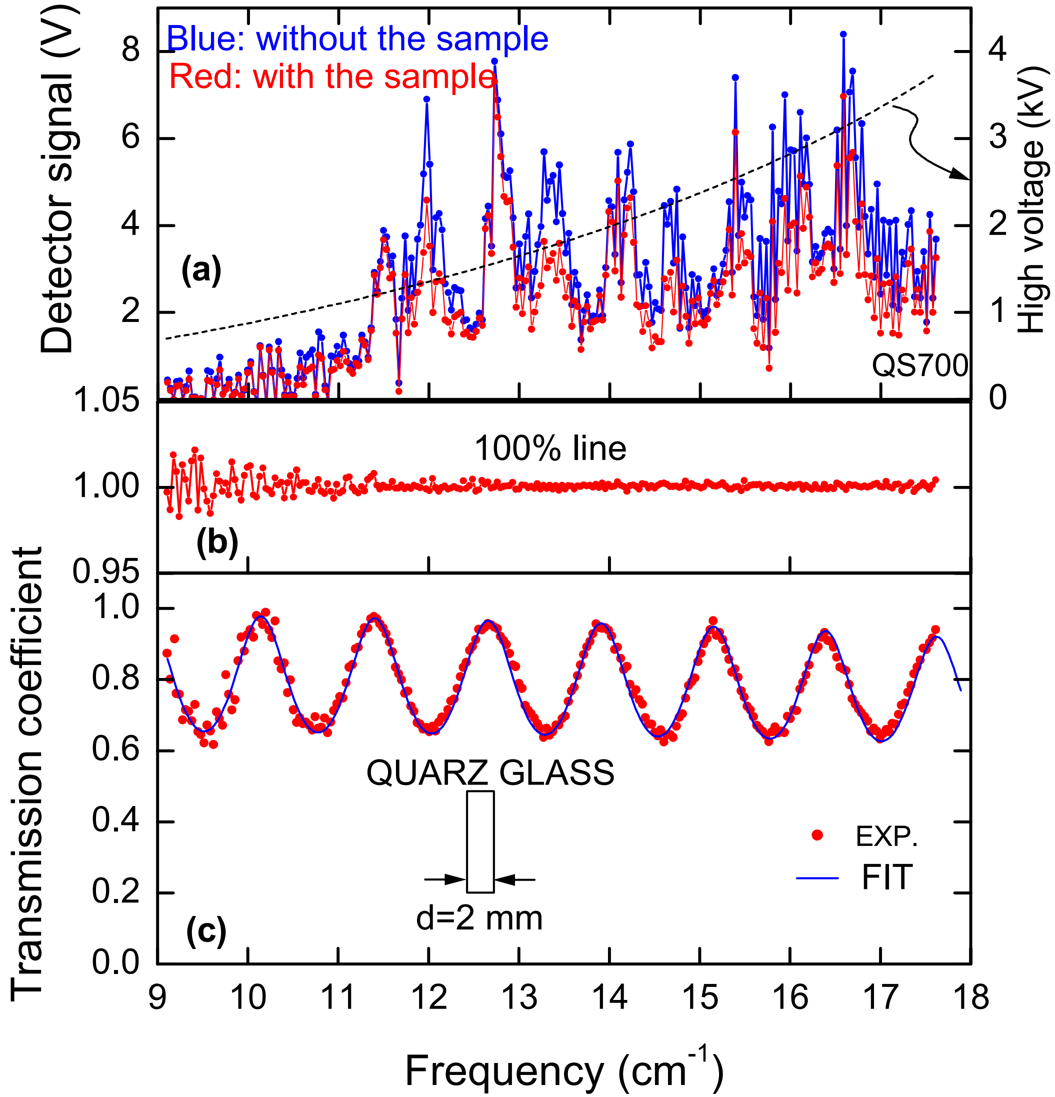

Spectroscopy of Mn_{12}*ac*

transmission and phase spectra

By measuring the **transmission and the phase**, the real and imaginary part of the permeability can be directly calculated at any frequency.

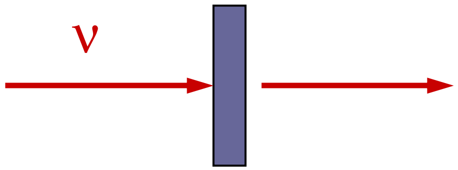

Absorption due **magnetic dipole transitions** between different energy levels split by the crystal field.

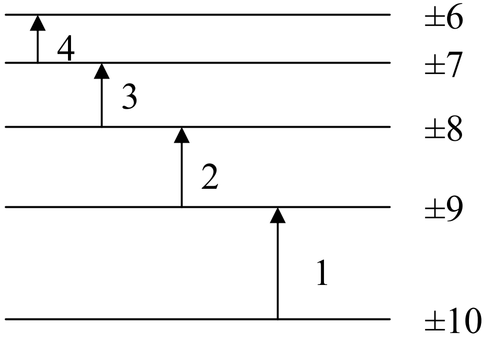

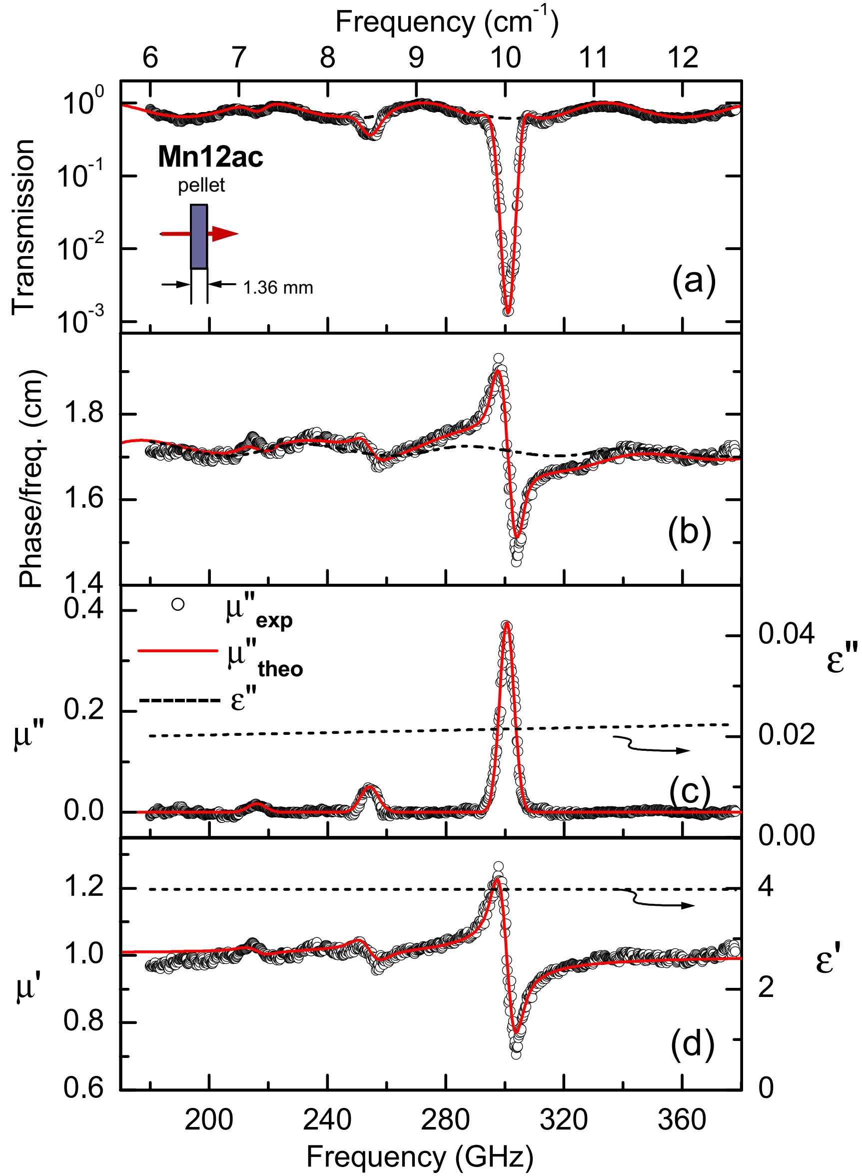

Spectroscopy of $Mn_{12}ac$

absorption lines in transmission spectra

For a good description we need
fourth order terms in the Hamiltonian:

$$H = DS_z^2 + E(S_x^2 - S_y^2) + \mathcal{O}^4$$

The **temperature dependent population** leads to contributions of higher states as the temperature increases:
$\Delta\,\mu \propto \exp\{-E/k_BT\}$.

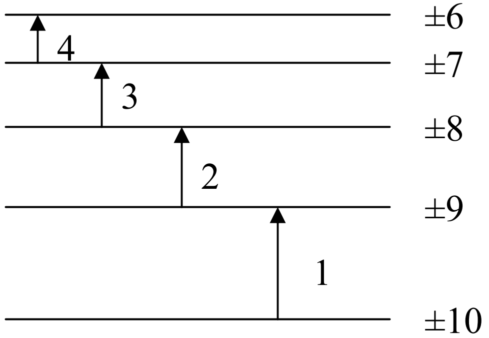

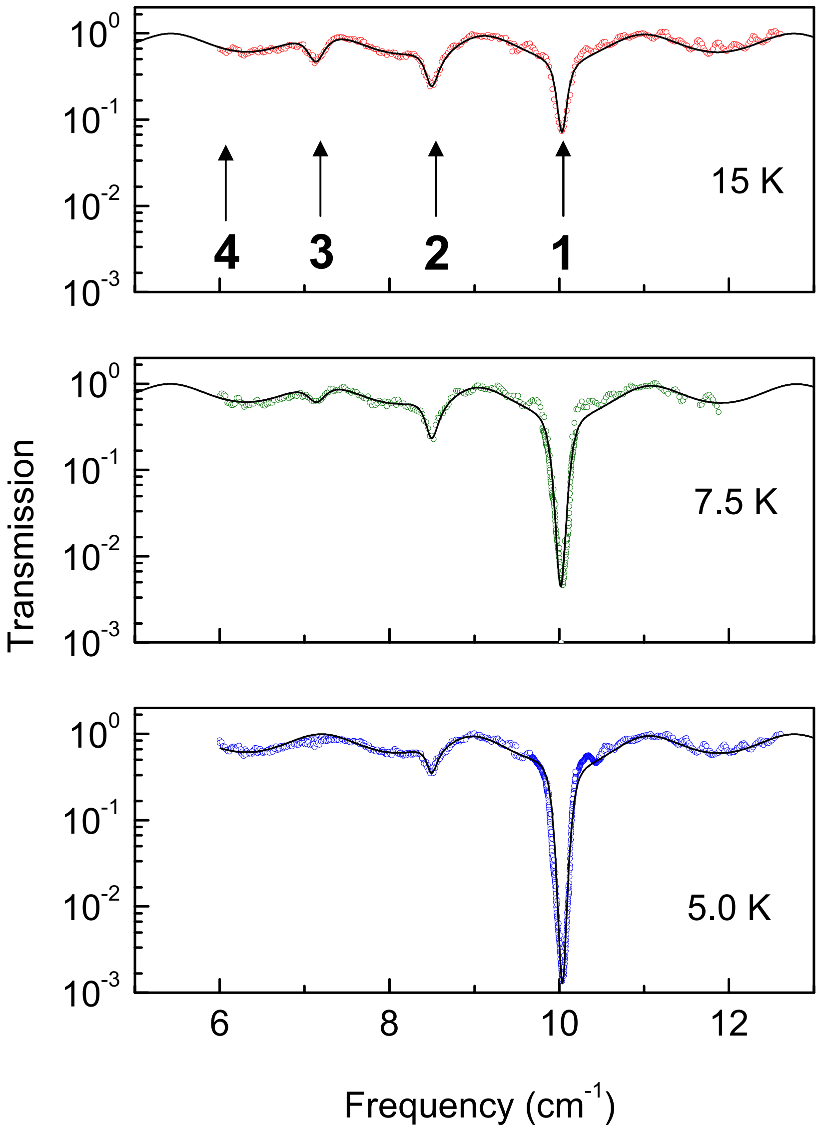

Spectroscopy of Mn_{12}*ac*

absorption lines in transmission spectra

The absorption spectra can be fitted by a **Gaussian line** shape rather than a Lorentzian line shape.

This holds for Mn_{12}*ac* as well as for other molecular magnets, like Fe_8.

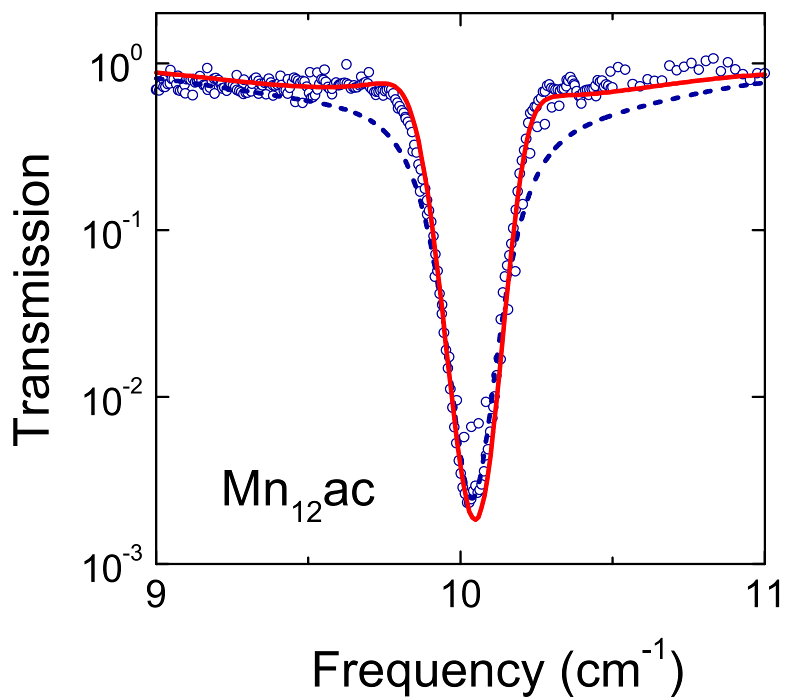

The **inhomogeneous broadening** may be due to the random distribution of the internal dipolar magnetic field.

It can be described by a variation of *D* (*D*-strain).

A. Mukhin et al. 1998, 2001

Spectroscopy of Mn_{12}*ac*
absorption lines in transmission spectra

Homogeneous broadening:
effect which is the same for each molecule.
- lifetime of the excited state.
- thermal vibrations.
- radiation damping.

Leads to **Lorentzian** lineshape.

Inhomogeneous broadening:
effect which is not the same for each molecule:
Distribution in:
- D parameter (D strain).
- E parameter.
- Internal dipolar fields.
- Easy axis direction.
- g value (g strain).

Leads to **Gaussian** lineshape.

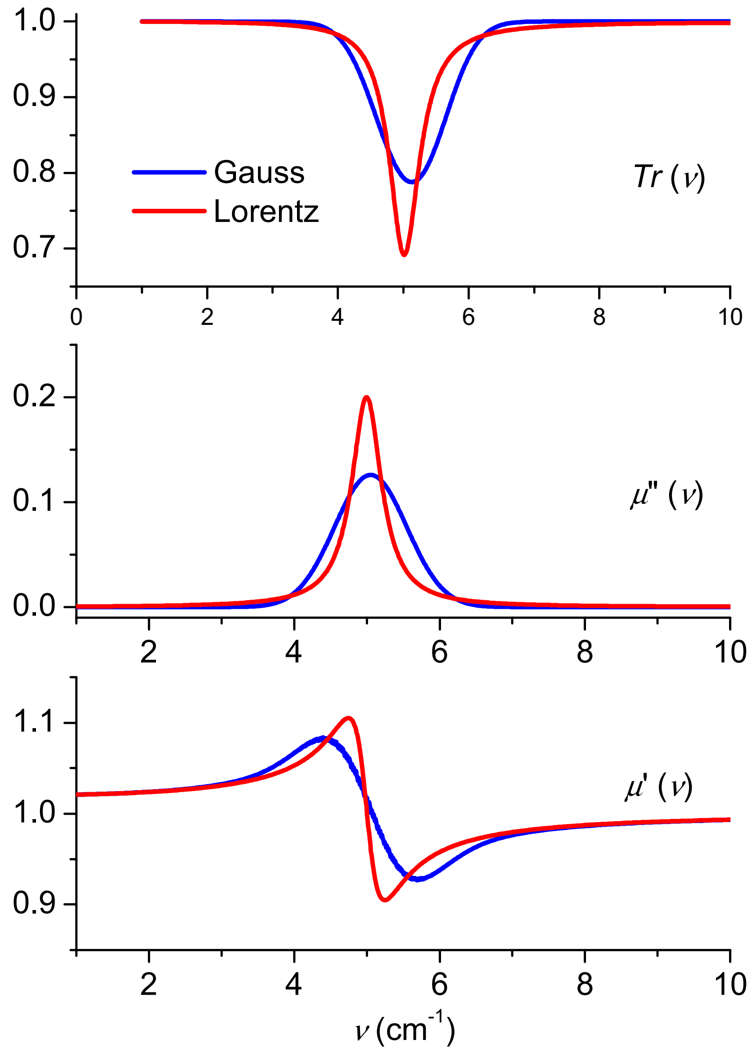

What happens
if an external magnetic field is applied?

Energy Levels
single spin model

Spin Hamiltonian

$$H = DS_z^2$$

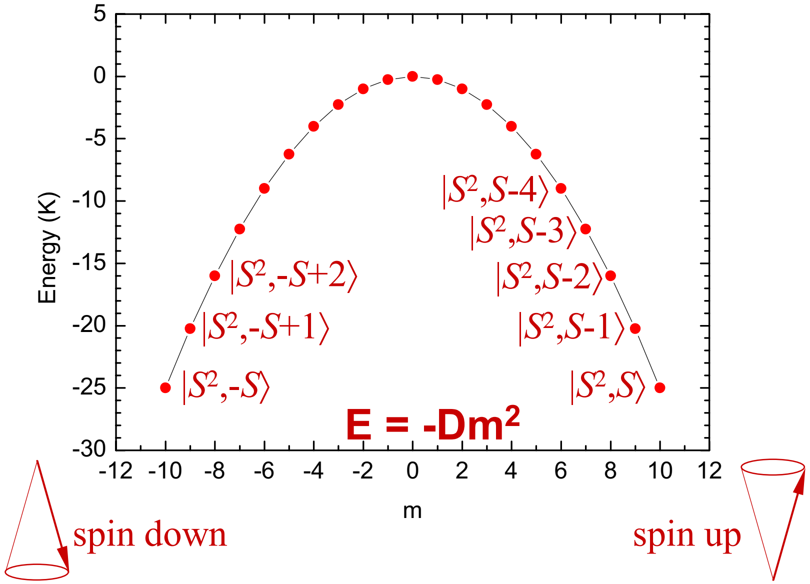

What happens
if an external magnetic field is applied ?

The energy levels for the two spin orientations and the barrier height change continuously with magnetic field B.

$$H = DS_z^2 + g\,\mu_B S \cdot B_0$$

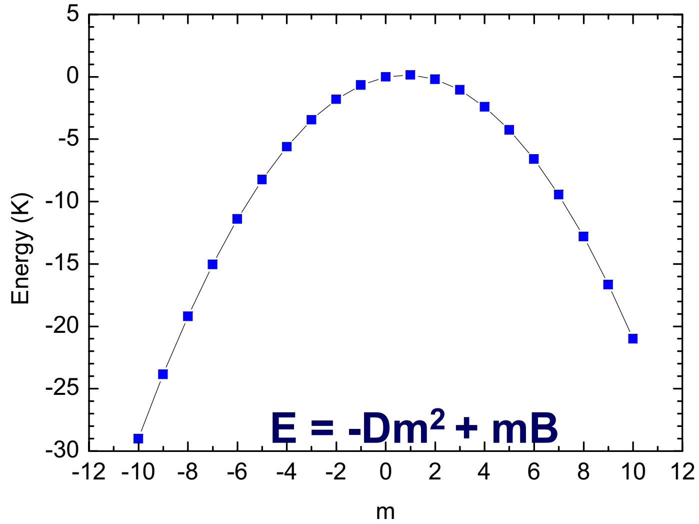

Influence of Magnetic Field

spectroscopy of $Mn_{12}ac$

Magnetic field dependence

- For **single crystals** the line split and shift in a magnetic field due to **Zeeman interaction**.

For polarization z || $B_{ext} \perp B_{ac}$

$$E_m = Dm^2 + D_1 m^4 + g\mu_B mB$$

At higher fields the **intensities** of the high- and low-frequency lines are unequal due to relaxation of the magnetization and Boltzmann statistics.

The **linewidth** remains unchanged.

No evidence for distribution in *g* values (*g*-strain).

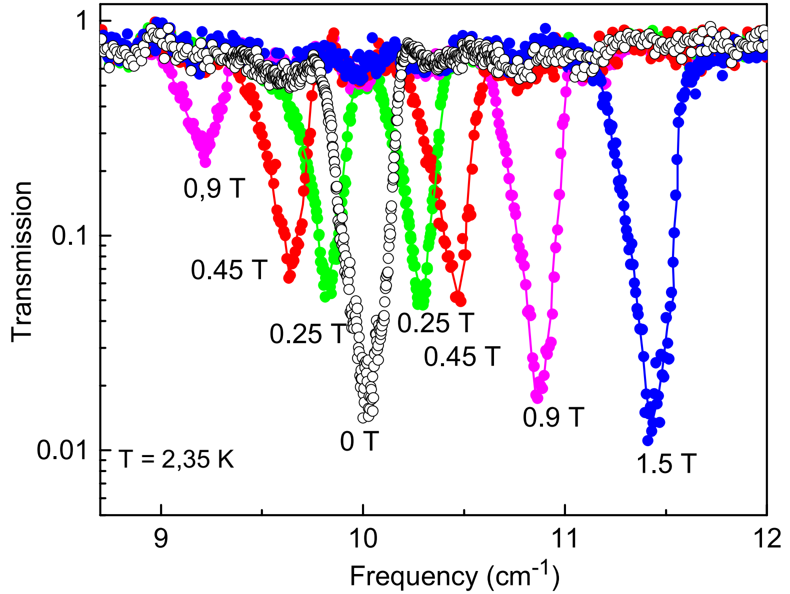

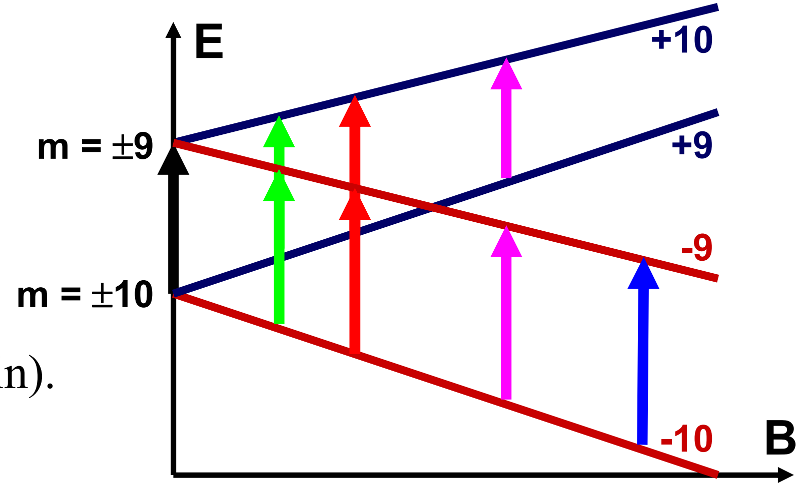

S. Vongtragool et al., Phys. Rev. B **69**, 104410 (2004)

Influence of Magnetic Field

powder samples

- For **polycrystalline samples** the lines broaden due to the distribution of the effective magnetic field

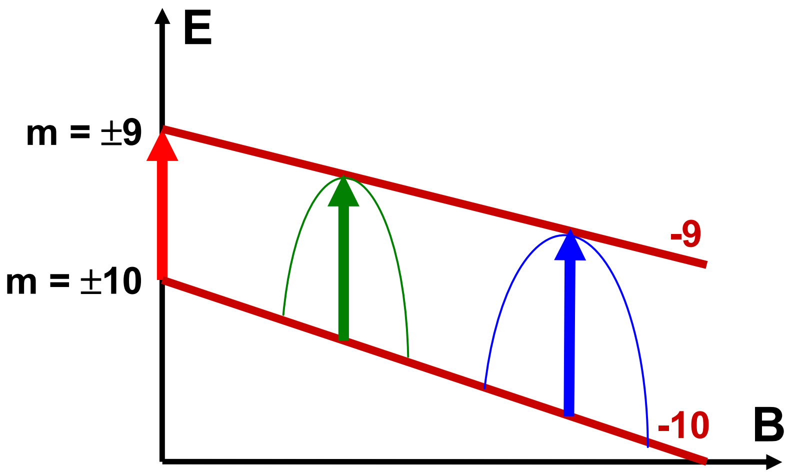

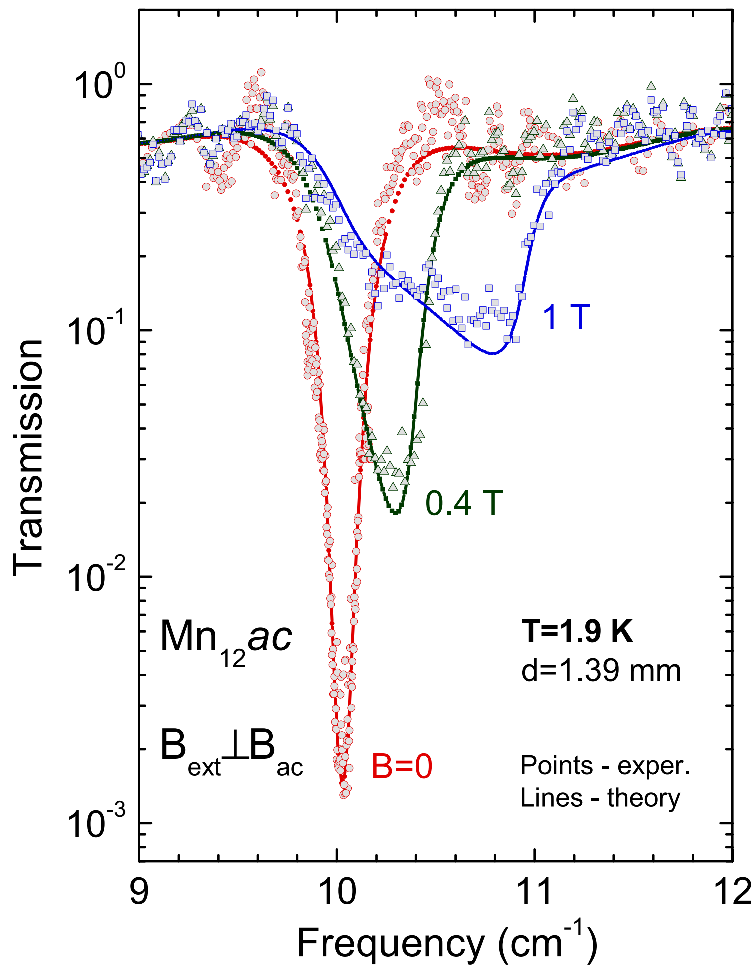

Influence of Magnetic Field

geometrical aspects

- Slightly different behavior for

Voigt configuration $q \perp B_{ext} \parallel z, \quad B_{ext} \parallel B_{ac}$

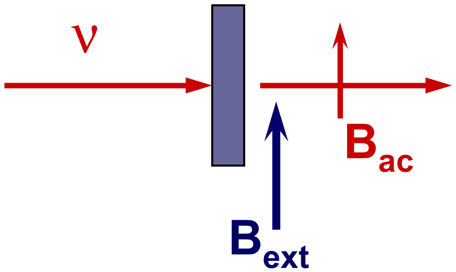

Voigt configuration $q \perp B_{ext} \parallel z, \quad B_{ext} \perp B_{ac}$

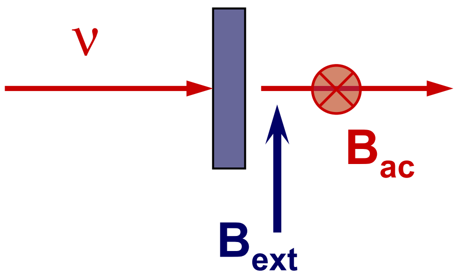

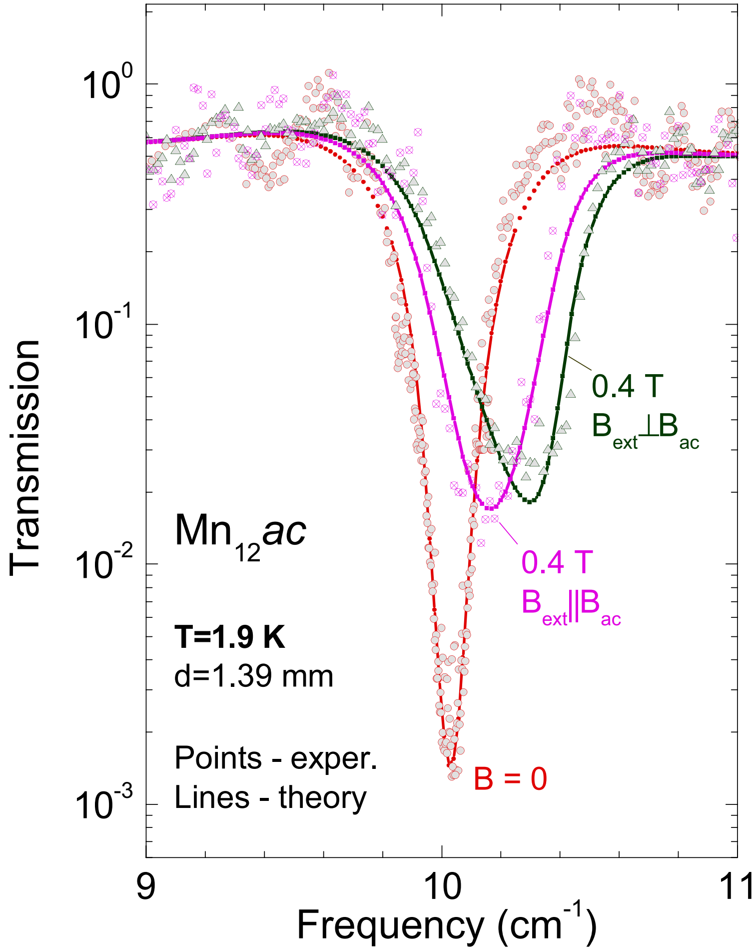

Influence of Magnetic Field

effective permeability

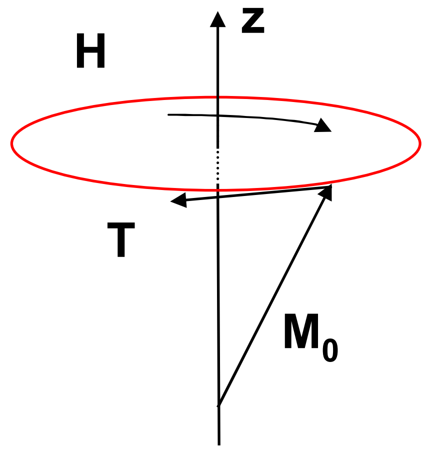

Torque: $\vec{\mathbf{T}} = \mu_0 \vec{\mathbf{M}} \times \vec{\mathbf{H}}$

Equation of motion: $\dfrac{d\vec{\mathbf{M}}}{dt} = \mu_0 \gamma \vec{\mathbf{M}} \times \vec{\mathbf{H}}$

AC field of radiation: $\vec{\mathbf{H}} = \vec{\mathbf{H}}_0 + \vec{\mathbf{h}}_{ac}$ $\quad \vec{\mathbf{M}} = \vec{\mathbf{M}}_0 + \vec{\mathbf{m}}_{ac}$

$\vec{\mathbf{M}} = \chi \vec{\mathbf{H}}$

Magnetic permeability tensor:
(from equation of motion)

$$\boldsymbol{\mu} = \mu_0 \begin{bmatrix} \mu & \kappa & 0 \\ \kappa & \mu & 0 \\ 0 & 0 & 1 \end{bmatrix}$$

with

$$\mu = 1 + \chi_{xx,yy} = 1 + \frac{\omega_0 \omega_m}{\omega_0^2 - \omega^2} \qquad \kappa = -i\chi_{xy} = i\chi_{yx} = \frac{\omega \omega_m}{\omega_0^2 - \omega^2}$$

Effective magnetic permeability:

Faraday geometry (M || q) $\quad \mu_{eff} = \mu \pm \kappa \quad$ ± depending on circular polarization

Voigt geometry (M ⊥ q) $\quad \mu_{eff} = \dfrac{\mu^2 - \kappa^2}{\mu}$

The transmission of a plane parallel sample
is a function of this effective magnetic permeability.

D.M. Pozar, Microwave Engineerin; B. Lax, K.J. Button, Microwave Ferrites and Ferrimagnetics

Voigt Configuration
effective permeability

- **zero-field cooled** *versus* **field cooled**
  On switching off the field,
  the absorption line does not coincide
  with the zero-field cooled one:
    - shift of line to higher frequency
    - change in line shape

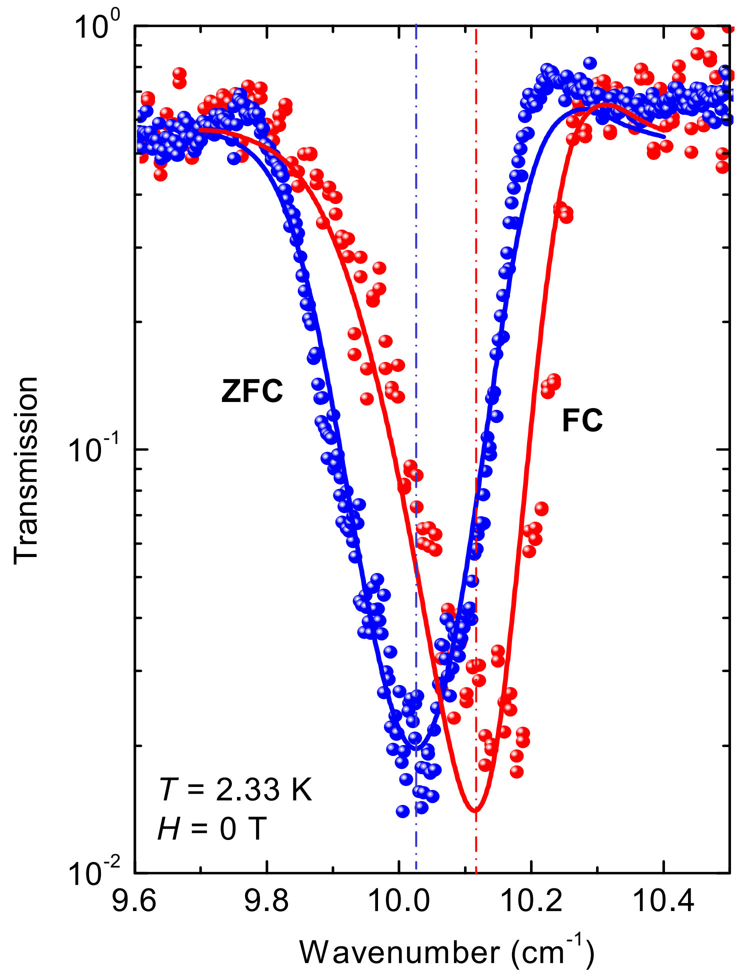

Due to the magnetization of the sample
the molecule feels an **internal magnetic field**:

$$H_{\text{eff}} = H_0 + \lambda M$$

Part of this shift is due to Zeeman term:

$$\tilde{\nu}^M = \tilde{\nu}^0 + g\mu_B \lambda M$$

Main part of shift is due to change in
effective permeability:

$$\mu_{eff}(\nu) = \mu_{xx}(\nu) - \frac{\mu_{xy}(\nu)\mu_{yx}(\nu)}{\mu_{yy}(\nu)}$$

$$\tilde{\nu}^M = \tilde{\nu}^0 \sqrt{1 + \Delta\mu}$$

Δμ is the mode contribution to the
magnetic permeability (transition probability).

S. Vongtragool et al., PRB **69**, 104410 (2004)

Voigt Configuration

effective permeability

- **zero-field cooled** *versus* **field cooled**
  On switching off the field,
  the absorption line does not coincide
  with the zero-field cooled one:
  - shift of line to higher frequency
  - change in line shape

ZFC line is symmetric Gaussian;
inhomogeneous broadening due to
random dipolar fields and distribution in *D*.

FC line is asymmetric Gaussian;
asymmetry due to combination of
magnetized sample

$$\mu_{eff}(\nu) = \mu_{xx}(\nu) - \frac{\mu_{xy}(\nu)\mu_{yx}(\nu)}{\mu_{yy}(\nu)}$$

and inhomogeneously broadened line.
It only occurs for Gaussian lineshape.

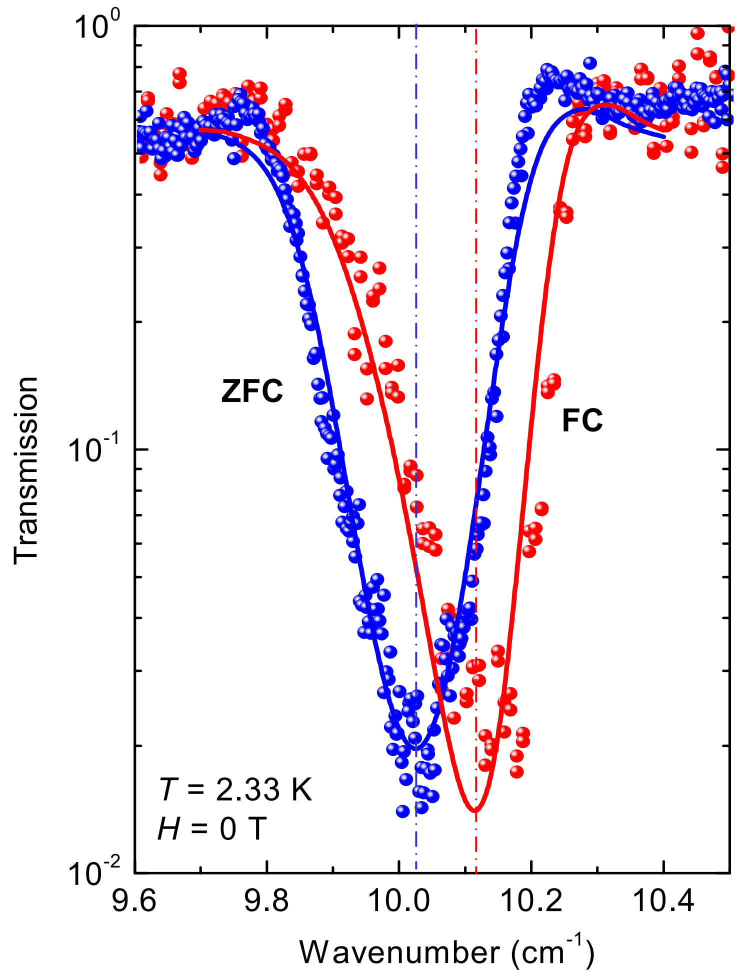

S. Vongtragool et al., PRB **69**, 104410 (2004)

Voigt Configuration
influence of magnetic field

- **asymmetric line shape**
  The asymmetry remains
  if the measurements are performed
  in external magnetic field and
  the absorption line shifts up in frequency.

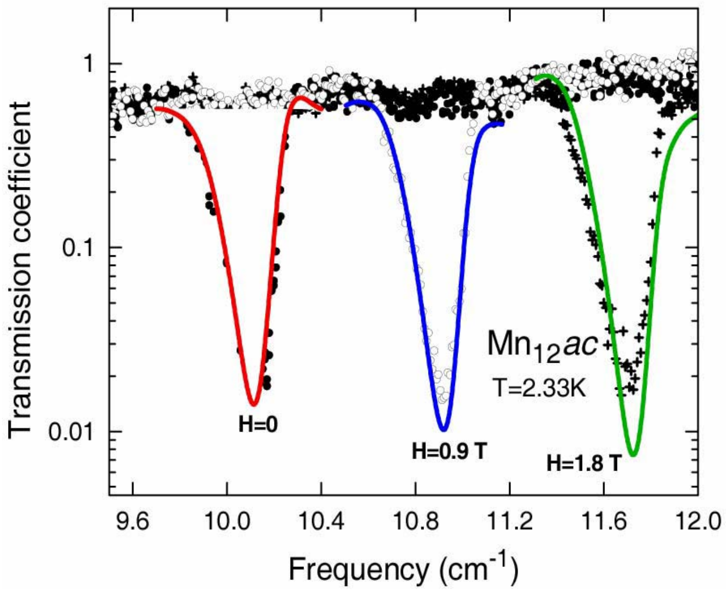

S. Vongtragool et al., PRB **69**, 104410 (2004)

Voigt and Faraday Configurations

geometrical aspects

- **Voigt configuration**

  $q \perp z \parallel B_{ext}, \quad B_{ext} \perp B_{ac}$

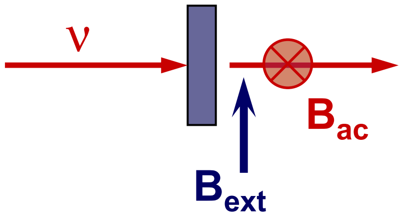

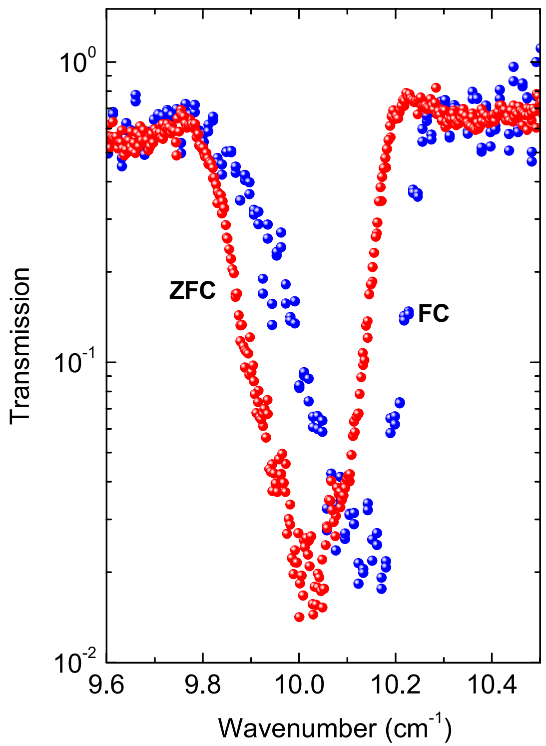

Faraday configuration

$q \parallel z \parallel B_{ext}$

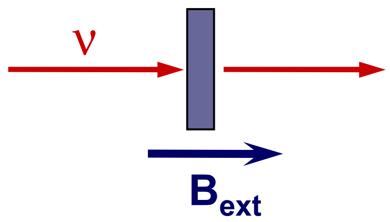

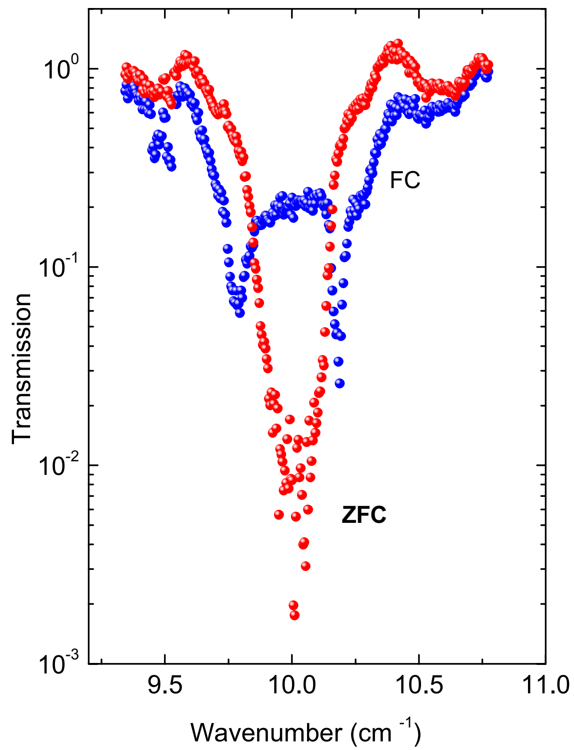

J. van Slageren et al. (2005)

Faraday Configuration
circular polarization

creation of circular polarized light

- Linearly polarized (45°) light
  falls on wire grid/mirror combination.
- Vertical component is transmitted at wire grid.
  Horizontal component is reflected at wire grid.
- A path length difference of λ/4 results in circular polarization.

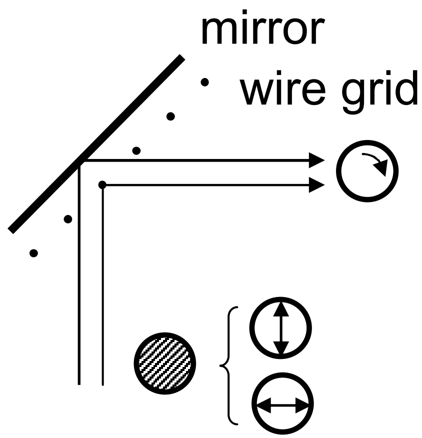

The degree of polarization $P = \frac{I_{\min}}{I_{\max}}$

P > 99 % at the center frequency

P > 80 % in a range ± 6 GHz

J. van Slageren et al. (2005)

Faraday Configuration
circular polarization

circular polarized light

- We can selectively excite states at only **one side of the barrier** according to ESR selection rules.

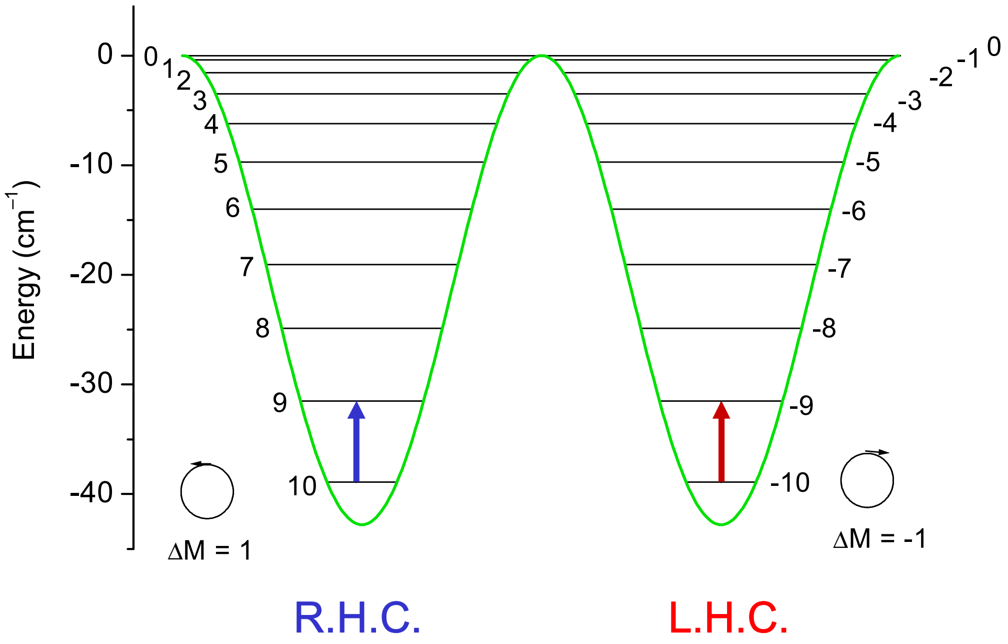

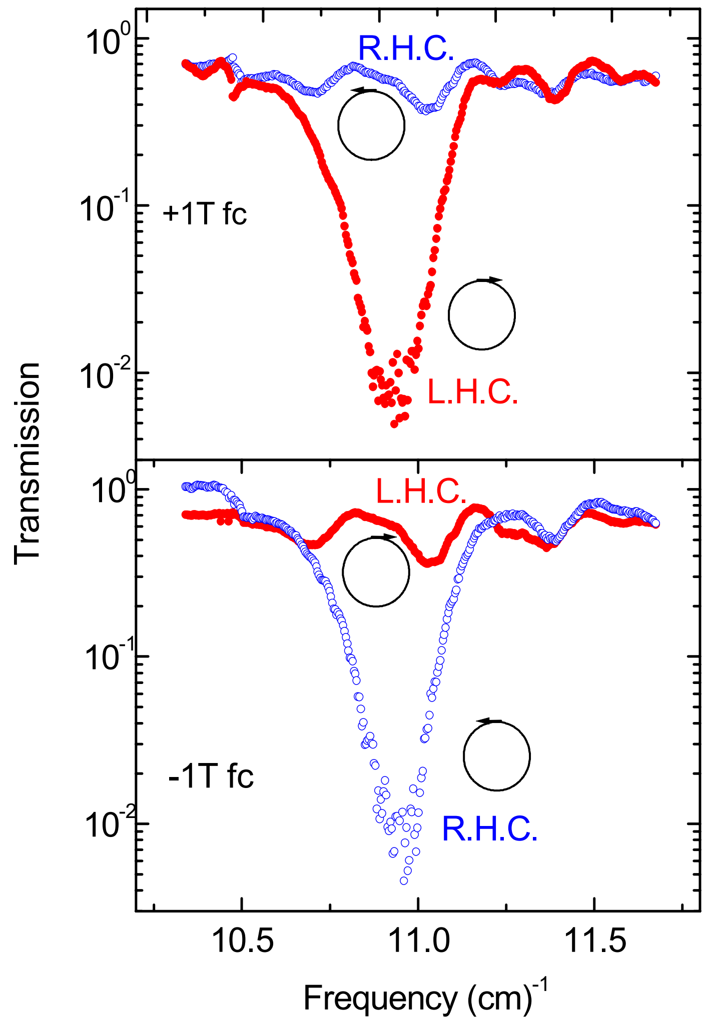

J. van Slageren et al. (2005)

Faraday Configuration
linear polarization

zero-field cooled *versus* **field cooled**

The effect of the off diagonal element is much stronger in Faraday geometry.

- Linearly polarized light can be decomposed into two circularly polarized waves: left handed and right handed poralized.
- Effective permeability (**M** along +**q**):
  left handed:
  $$\mu_{eff} = \mu - \kappa$$
  right handed:
  $$\mu_{eff} = \mu + \kappa$$
- These two waves interfere, giving strange lineshape if the analyzer is at θ = 0°
  $$Tr = abs\left(\frac{t^+ + t^-}{2}\right)^2$$

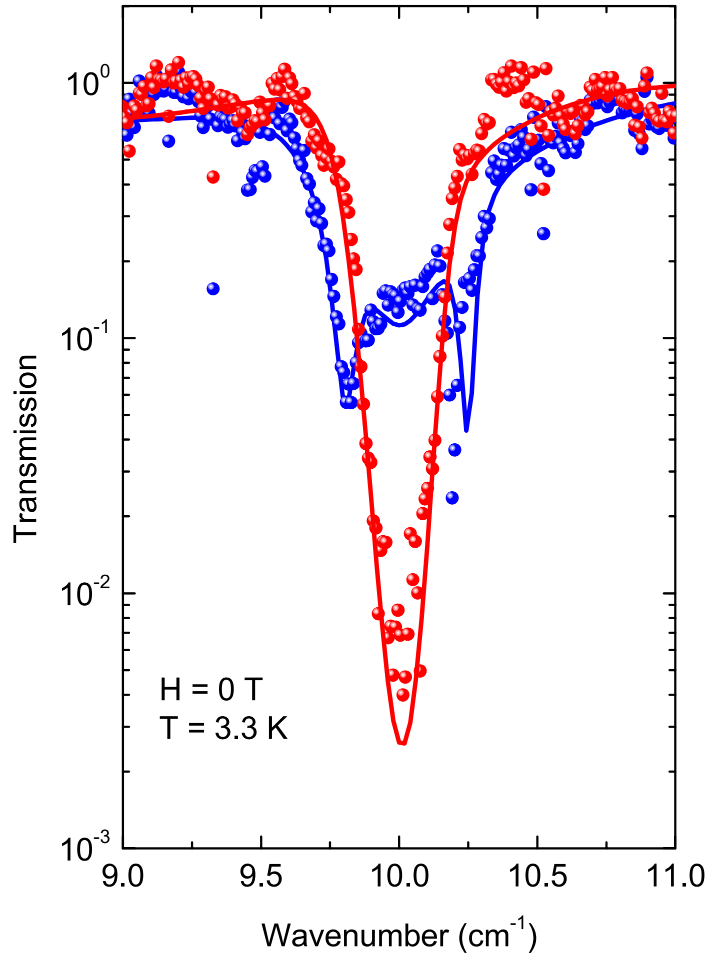

J. van Slageren et al. (2005)

Faraday Configuration
linear polarization

angle of polarization

The transmission spectra of magnetized crystals very much depend on the angle α between polarizer and analyzer.

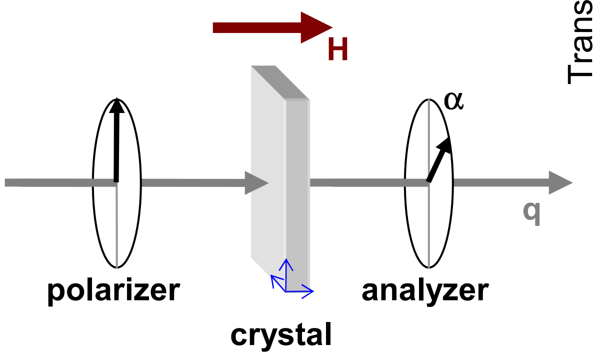

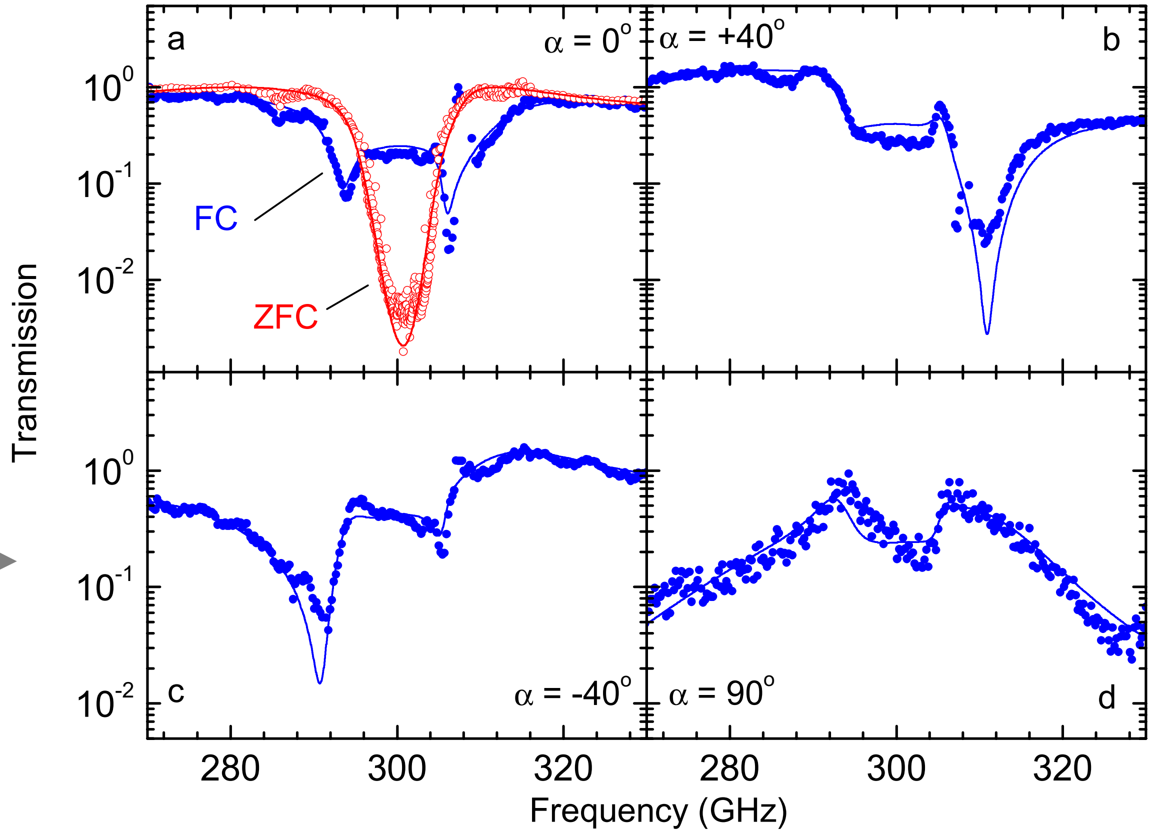

The complicated behavior can be fully described by the effective permeability tensor.

J. van Slageren et al. (2005)

Faraday Configuration

linear polarization

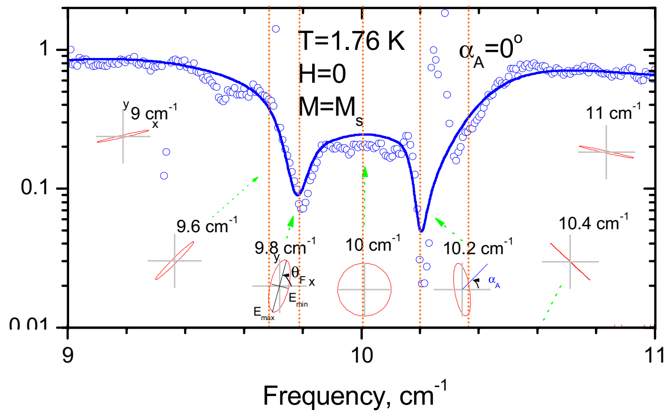

angle of polarization

- at resonance (10 cm^{-1}) only one component of the circular polarized radiation is absorbed, the other is transmitted: 50% signal, circular polarized.
- at the edges both component have a phase shift leading to a rotation of the polarization ellipse.
- if the phase shift is 90°, the transmission is minimum.

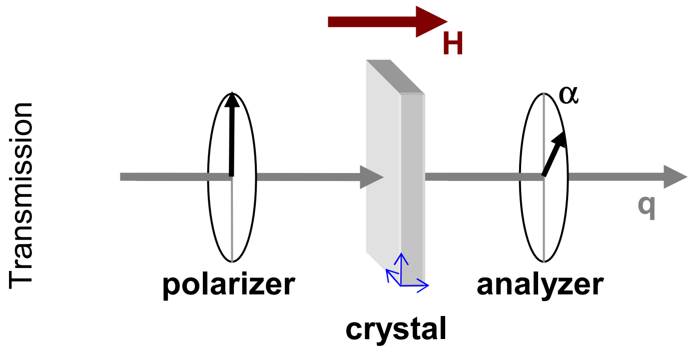

- rotating the analyzer by $\alpha_A = 90°$, leads to maximum transmission at the corresponding frequencies.

Faraday Configuration

linear polarization

angle of polarization

- with the analyzer rotated
  to some intermediate angles ($\alpha_A = \pm 40\,°$)
  the polarization state for each frequency
  can be probed.

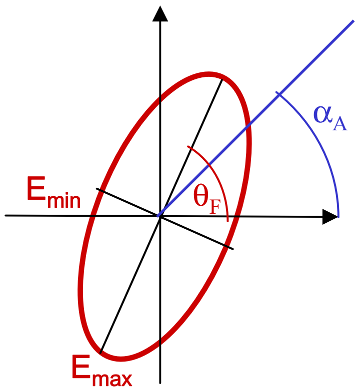

The **Faraday angle θ_F** describes the rotation of the polarization ellipse.

The **ellipticity** describes the ratio $\mathbf{E_{min}/E_{max}}$.

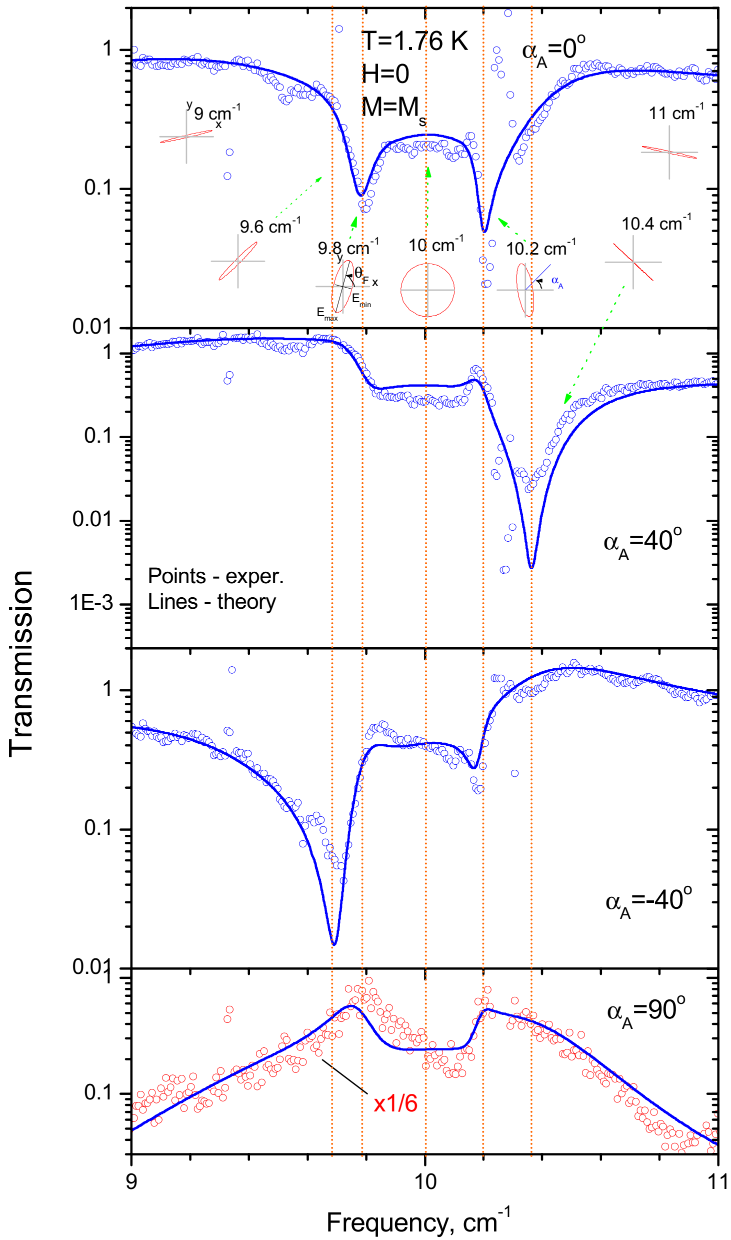

Faraday Configuration

linear polarization

Faraday rotation

The Faraday angle
and the ellipticity
changes with frequency
upon passing through the
absoption line.

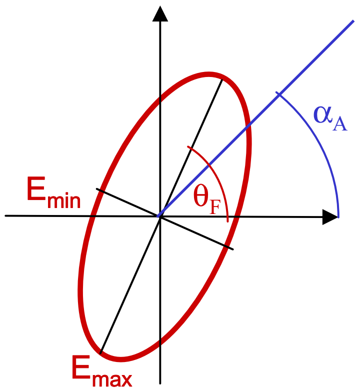

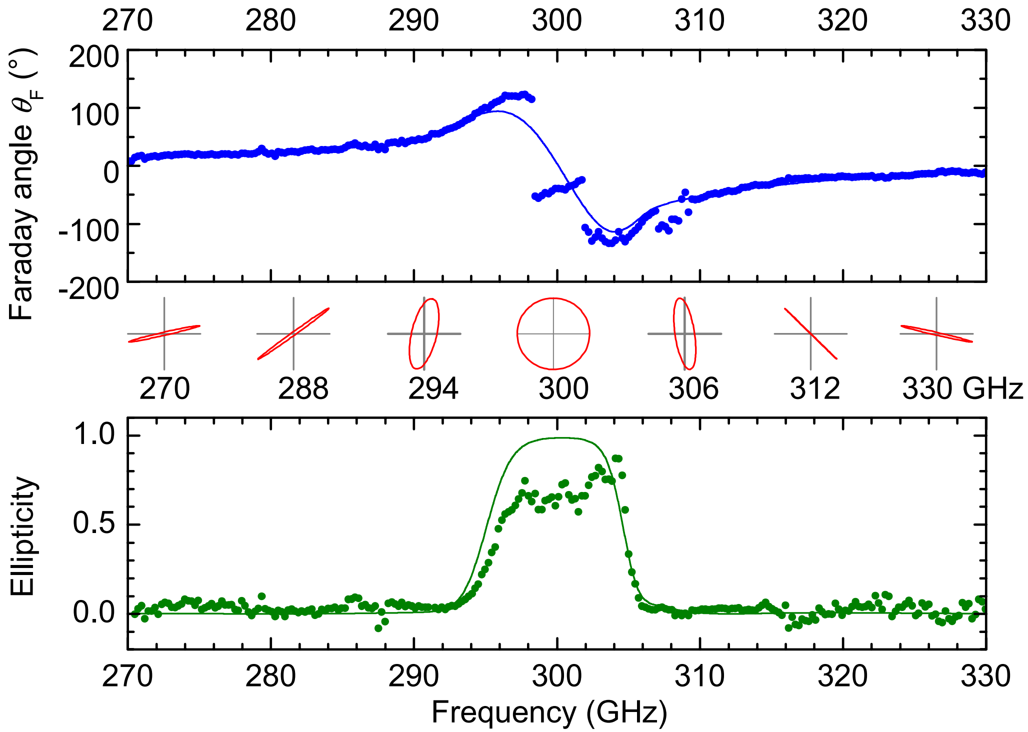

The Faraday rotation is strongest
near the magnetic resonance of the single molecule magnet $Mn_{12}Ac$ at ν = 300 GHz,
where the Faraday rotation exceeds **150°/mm**.
This is among the largest Faraday rotations ever observed.

J. van Slageren et al. (2005)

Faraday Configuration

linear polarization

dependence on magnetic field

Even for ZFC samples the transmission spectra exhibit the double-peak structure for finite external field.

This is explained by the fact that the |+10⟩→|+9⟩ and |-10⟩→|-9⟩ transitions are split up.
The radiation shows the Faraday effect around both resonances.

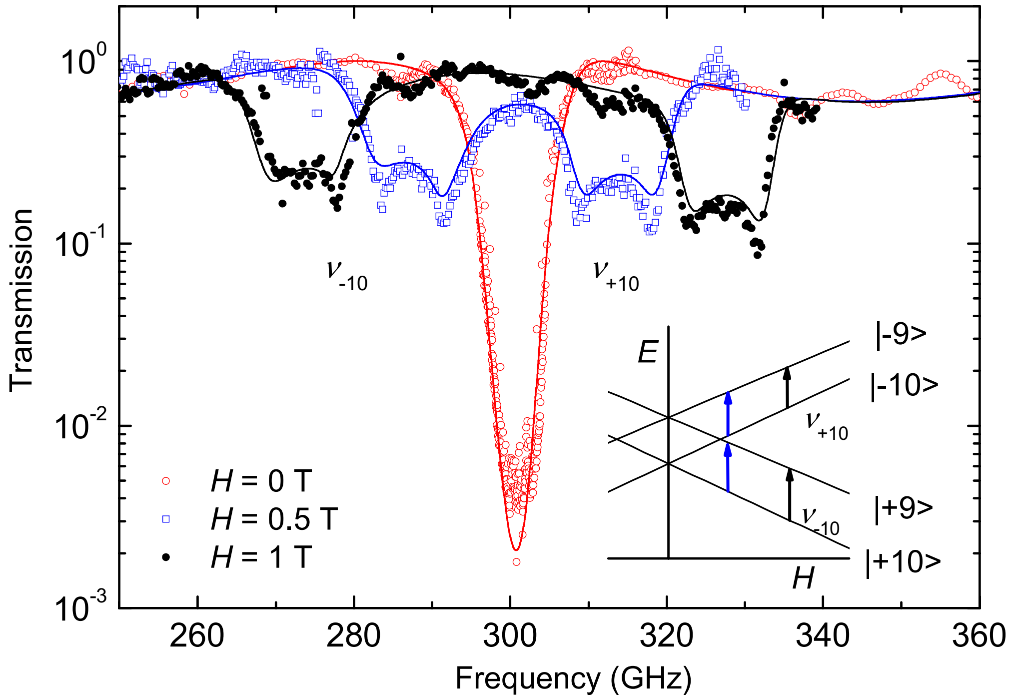

This is the first observation of a **Faraday effect in non-magnetized media**.
The Faraday rotation is not proportional to the overall sample magnetization.

J. van Slageren et al. (2005)

What happens
if the magnetic field changes?

Relaxation Processes

spectroscopic investigations

Magnetic field dependence of energy levels

$$E_m = Dm^2 + D_1 m^4 + g\mu_B mB$$

1. **Original state**
   Magnetic field B = 0
   $|\pm 10\rangle \rightarrow |\pm 9\rangle$
2. **Polarization of spins**
   Magnetic field B = 0.4 T
   $|+10\rangle \rightarrow |+9\rangle$
3. **Detection of transitions**
   Magnetic field B = -0.4 T
   $|+10\rangle \rightarrow |+9\rangle$
4. **Relaxation**
   Magnetic field B = -0.4 T
   $|-10\rangle \rightarrow |-9\rangle$

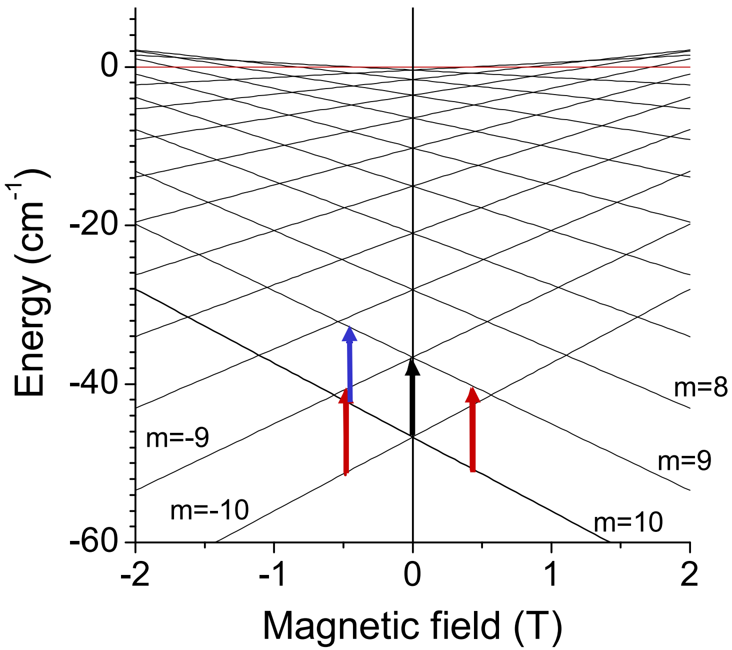

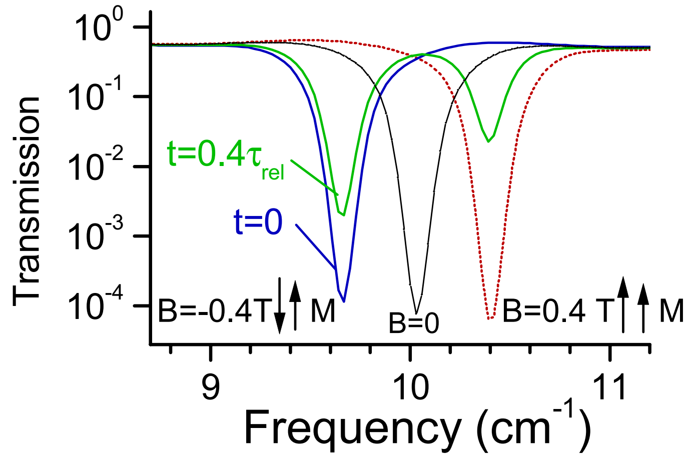

Relaxation Processes

time dependent population

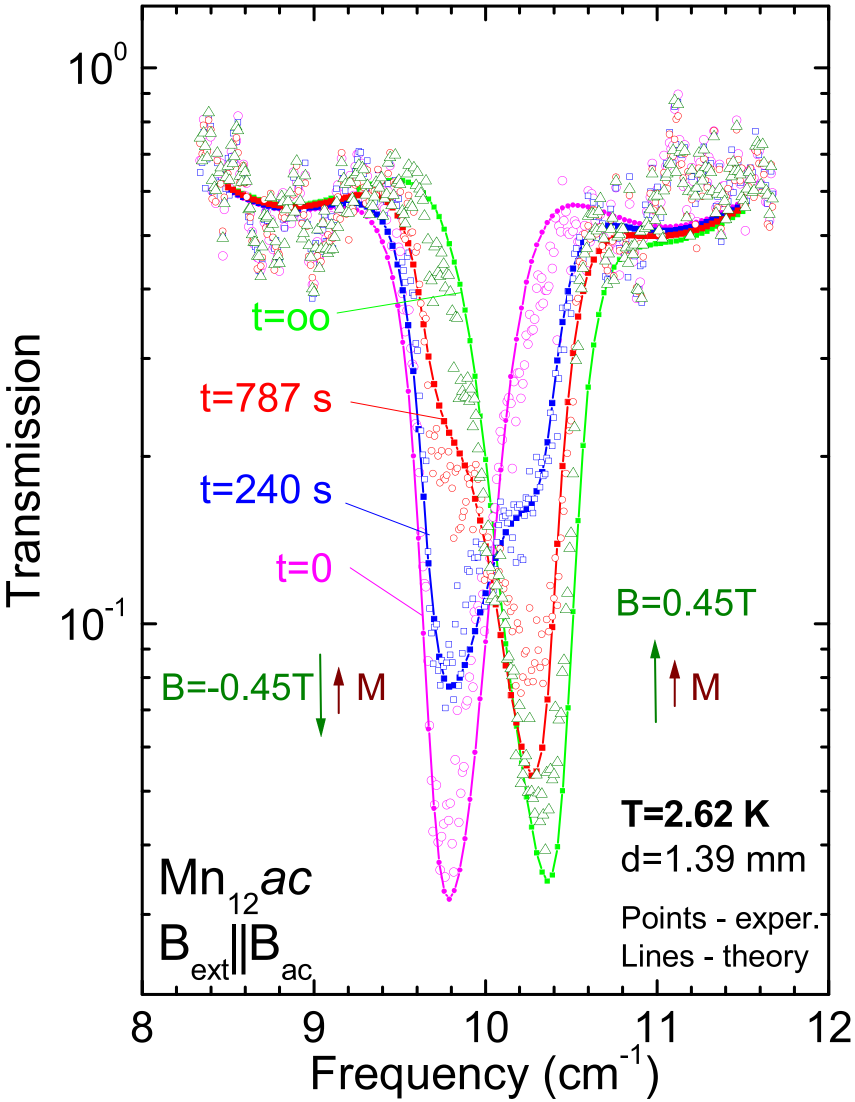

Reversing the magnetic field B leads to an inversion of population.

Relaxation of |10> state which was populated by B<0.

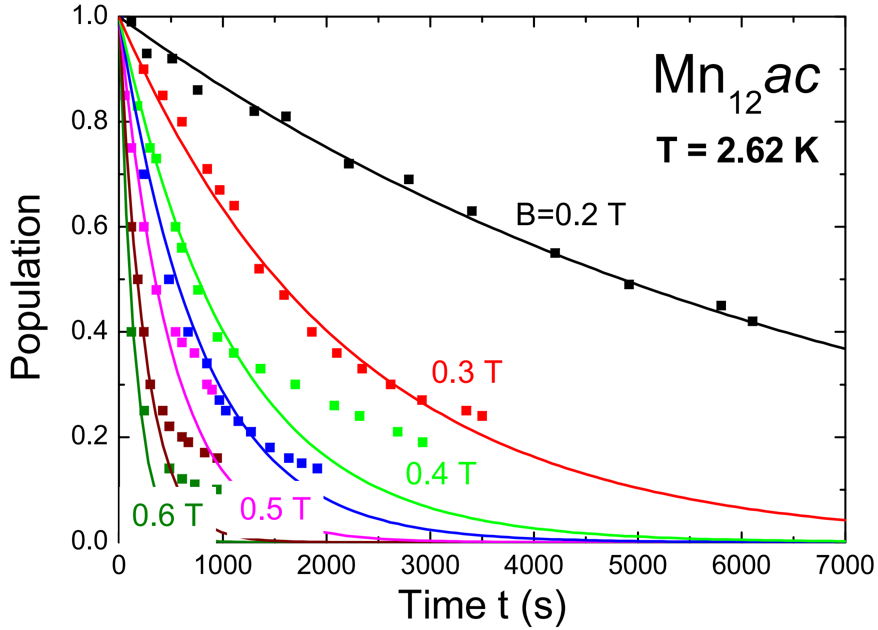

Fit of time dependent population

$$\Delta\mu \propto \exp\left\{\frac{-t}{\tau_{rel}}\right\}$$

Relaxation Processes

magnetic field dependence

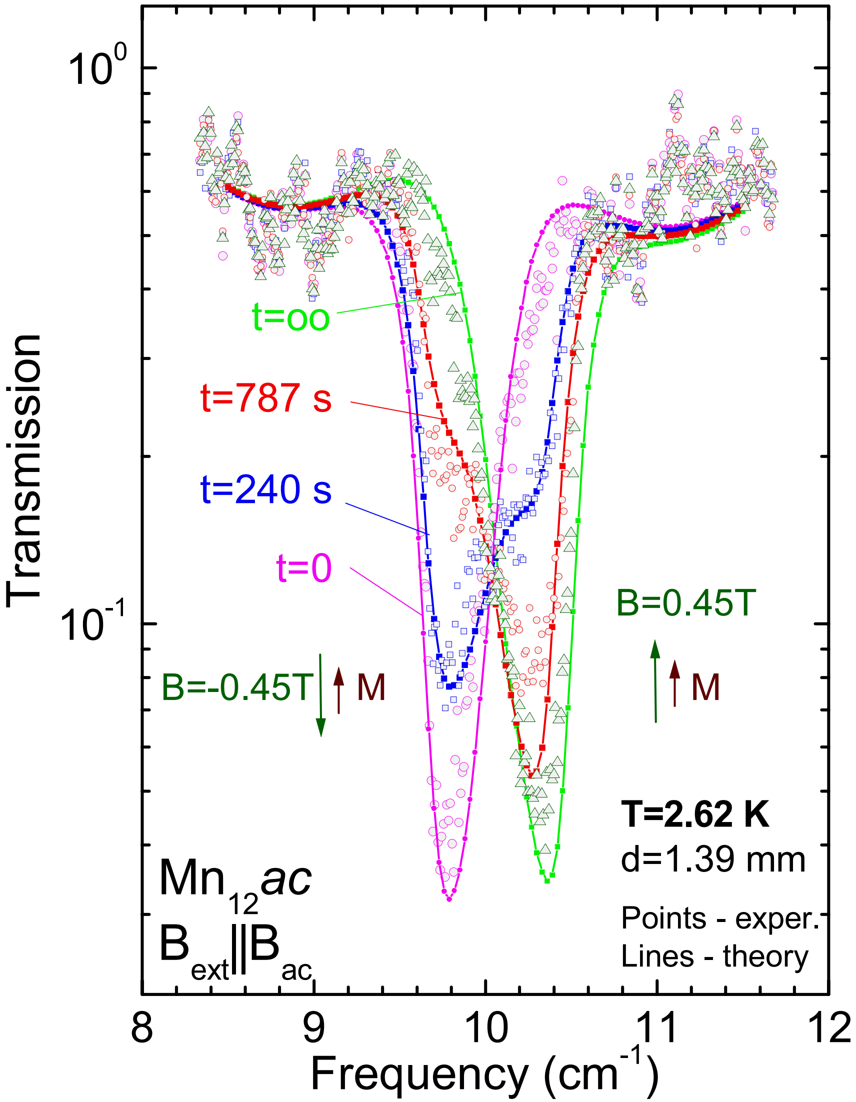

The relaxation time follows Arrhenius law

$$\tau = \tau_0 \exp\left\{ E_b^0 \frac{1-\alpha B / B_A}{T} \right\}$$

with $E_b^0=64$ K, $B_A=10$ T, $\tau_0=1.3 \cdot 10^{-6}$ s, $\alpha=4$

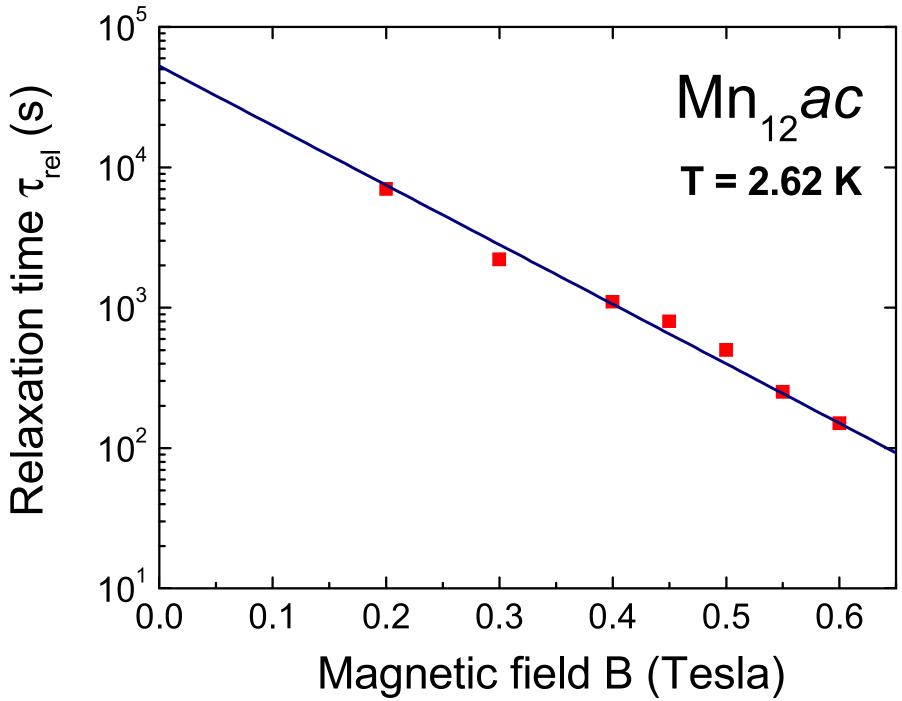

Magnetic Quantum Tunneling
single spin model

Transitions from one side to the other
are possible either

1. **thermally excited:** hopping over the barrier

2. **tunneling** between the ground states

3. **thermally assisted tunneling**
between excited states

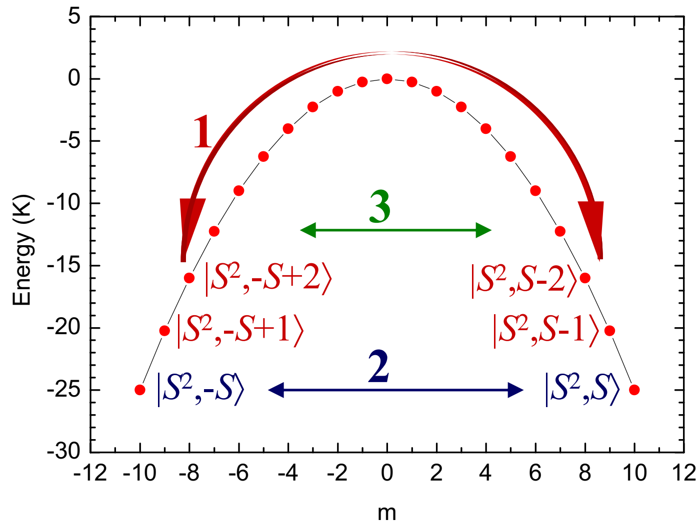

In the case of an external magnetic field B
the level crossing between
states ***E*(*m*)** and states ***E*(*n-m*)** occur at:

$B_n = nD/g\mu_B B\{1+B/D[(m-n)^2+m^2]\}$

Mn_{12}*ac*: $B_n = 0.45$ T

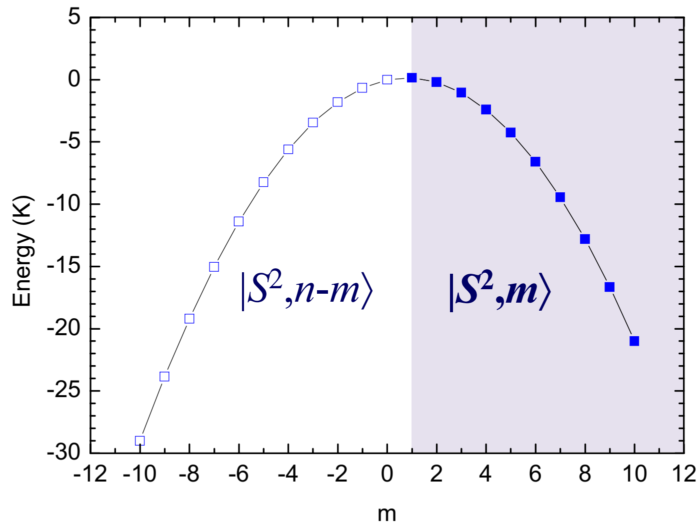

Magnetic Quantum Tunneling

symmetry of Hamiltonian

Tunneling of the magnetization is due to transverse terms in spin Hamiltonian.

$$H = DS_z^2 + BS_z^4 + C(S_+^4 + S_-^4)/2 + \mathcal{O}^4 + g\,\mu_B S\cdot B_0 \qquad S_\pm = S_x \pm iS_y$$

If this Hamiltonian is correct, the first transverse term is of fourth order and only tunneling between states with $\Delta m_S = \pm 4$ is allowed.

However all crossings are observed as steps in the hysteresis curve.

The presence of a second order transverse anisotropy could couple states with $\Delta m_S = \pm 2$.

The presence of a transverse magnetic field could couple states with $\Delta m_S = \pm 1$.

Clearly the proposed Hamiltonian is not complete.
Somehow the actual symmetry of the cluster is lower.

Magnetic Quantum Tunneling

symmetry of Hamiltonian

1. **Dislocations**
   Lead to a continuous distribution in anisotropy parameters

2. **Solvent disorder**
   CO crystallized acetic acid is disordered over two positions
   This leads to 6 discrete isomers,
   of which only two have tetragonal symmetry.

3. **Sample degradation**
   due to solvent loss.

4. **Transverse fields**
   due to misalignment.

Edge dislocation

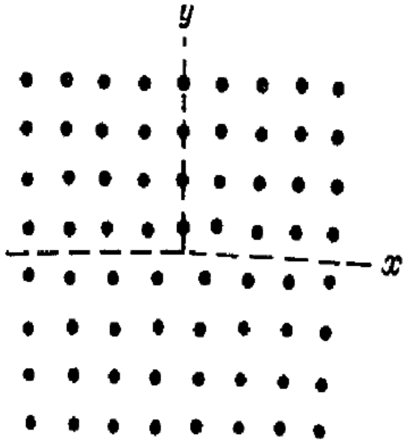

Screw dislocation

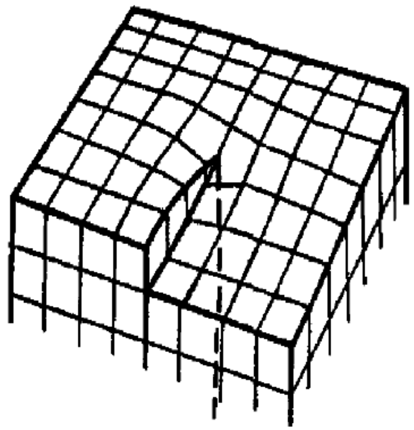

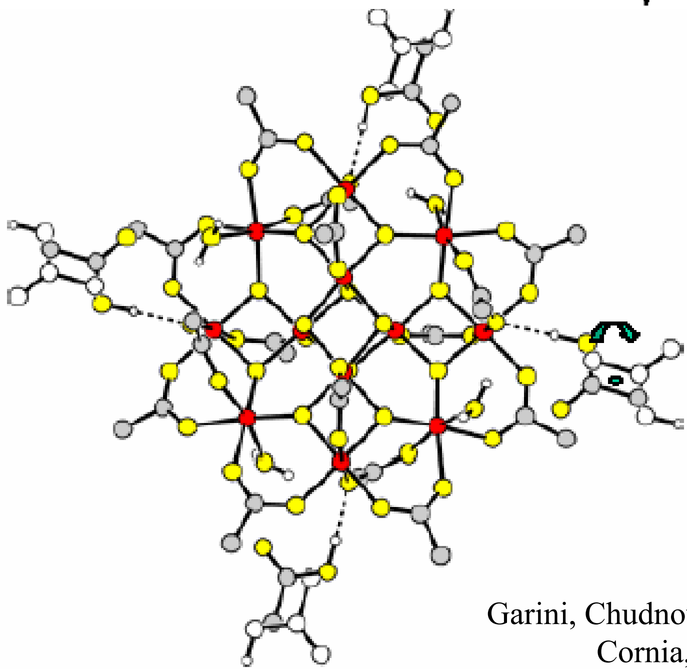

Garini, Chudnovsky, 2001
Cornia, et al 2002

How can we investigate the tunneling between two distinct levels?

Magnetization measurements are an integral method which summarize over all states.

We want to watch the change in population of a certain level as a function of magnetic field.

Magnetic Quantum Tunneling

spectroscopic investigations

Magnetic field dependence of energy levels

$$E_m = Dm^2 + D_1 m^4 + g\mu_B mB$$

1. **Original state**
   Magnetic field B = 0
   $|\pm 10\rangle \rightarrow |\pm 9\rangle$

2. **Polarization of spins**
   Magnetic field B = 0.9 T
   $|+10\rangle \rightarrow |+9\rangle$

3. **Detection of transitions**
   Magnetic field B = -0.9 T
   $|+10\rangle \rightarrow |+9\rangle$

4. **Relaxation**
   Magnetic field B = -0.9 T
   $|-10\rangle \rightarrow |-9\rangle$

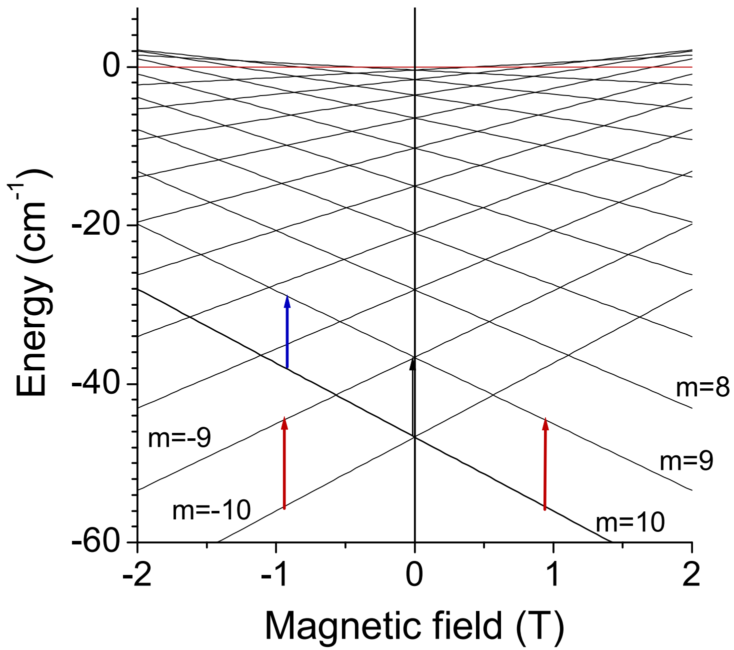

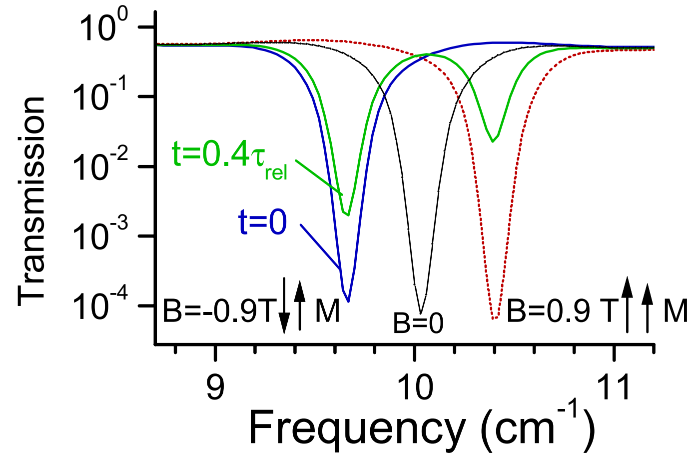

Magnetic Quantum Tunneling

spectroscopic hole burning

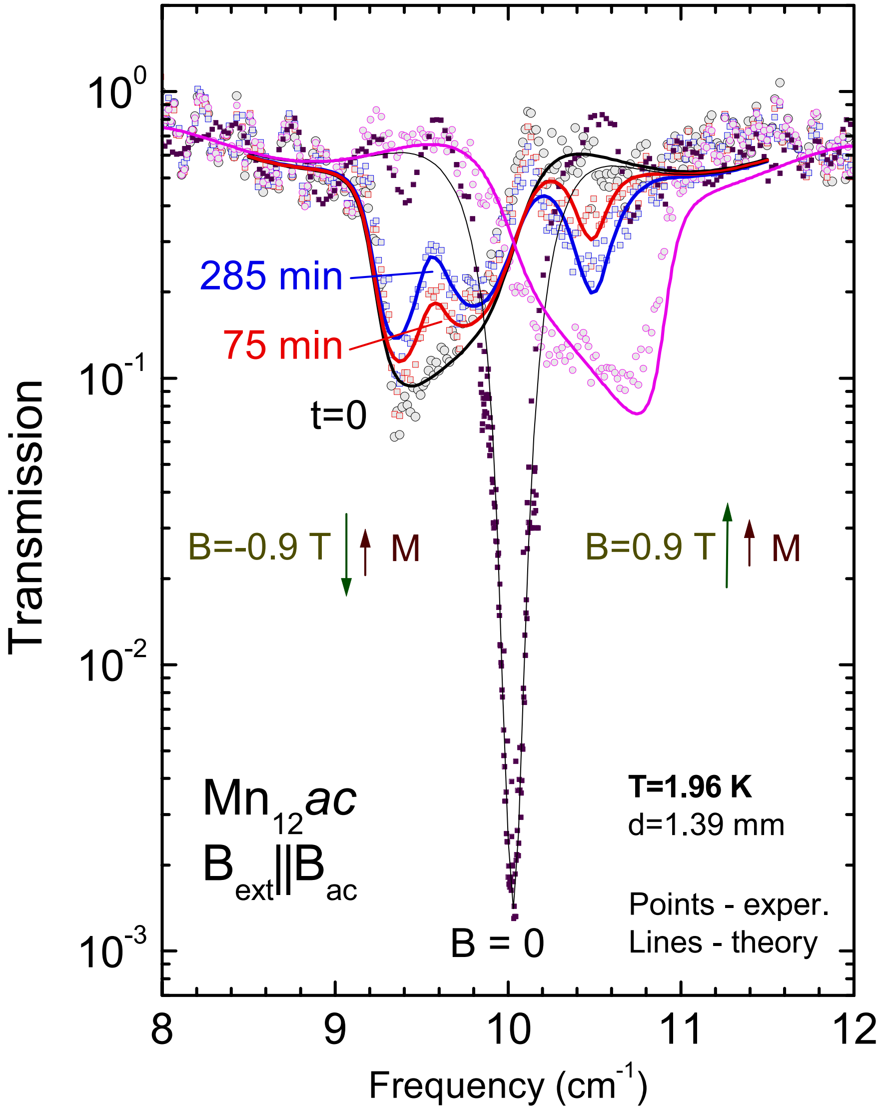

At the level crossing,
there is a faster relaxation path
which leads to
resonant quantum tunneling.

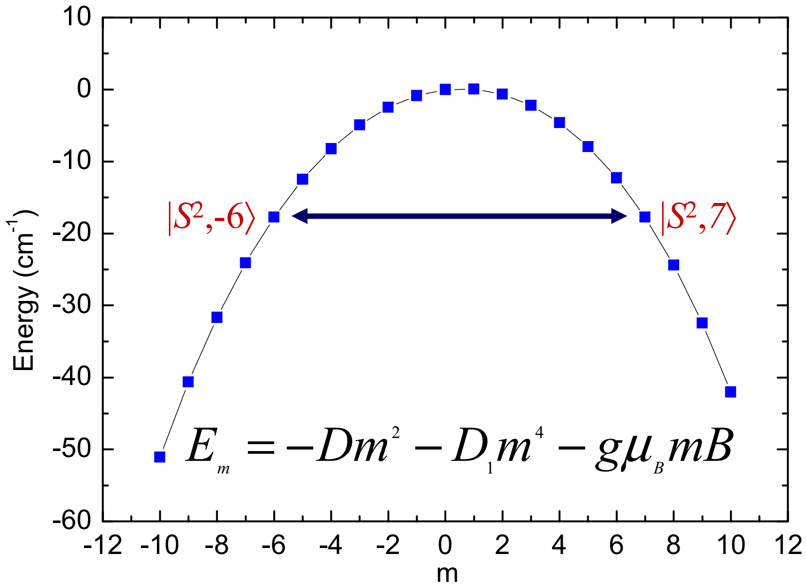

This causes a dip in the absorption band:
magnetic hole burning.

We describe the results **quantitatively** by a theoretical model (solid lines).

M. Dressel et al., Phys. Rev. B **67**, 060405(R) (2003)

Magnetic Quantum Tunneling

spectroscopic hole burning

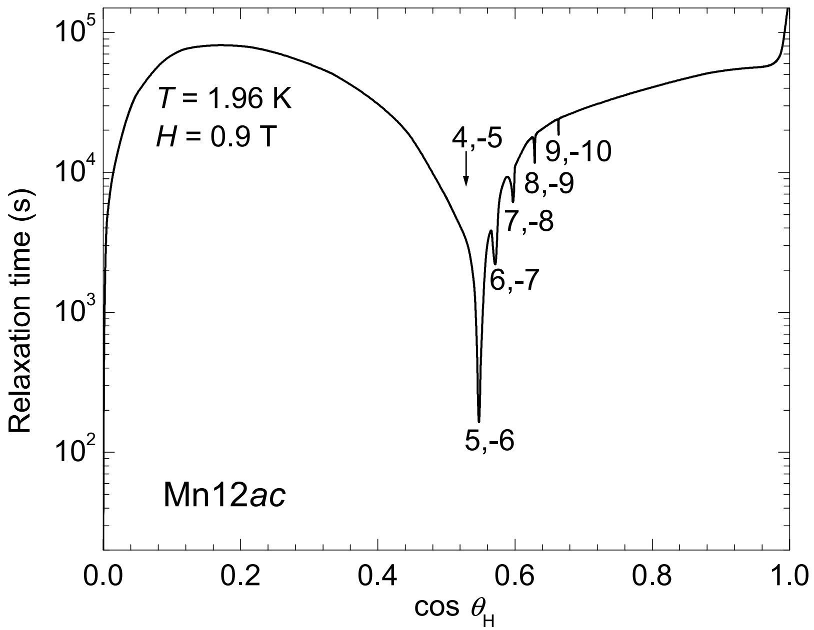

At the level crossing,
there is a faster relaxation path
which leads to
resonant quantum tunneling.

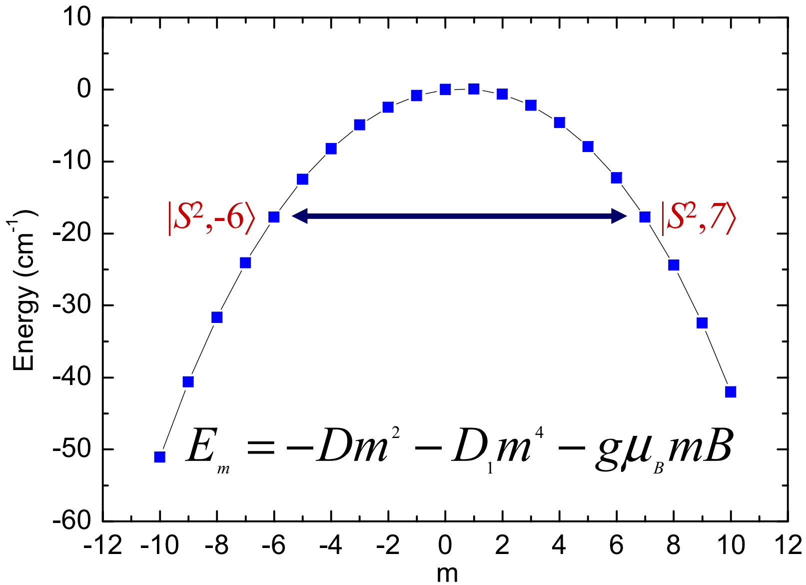

This causes a dip in the absorption band:
magnetic hole burning.

We describe the results **quantitatively** by a theoretical model (solid lines).

M. Dressel et al., Phys. Rev. B **67**, 060405(R) (2003)

Magnetic Quantum Tunneling

spectroscopic investigations

- In **single crystals**, the population of the ground level m = -10 can be studied as a function of time, leading to some relaxation rate.

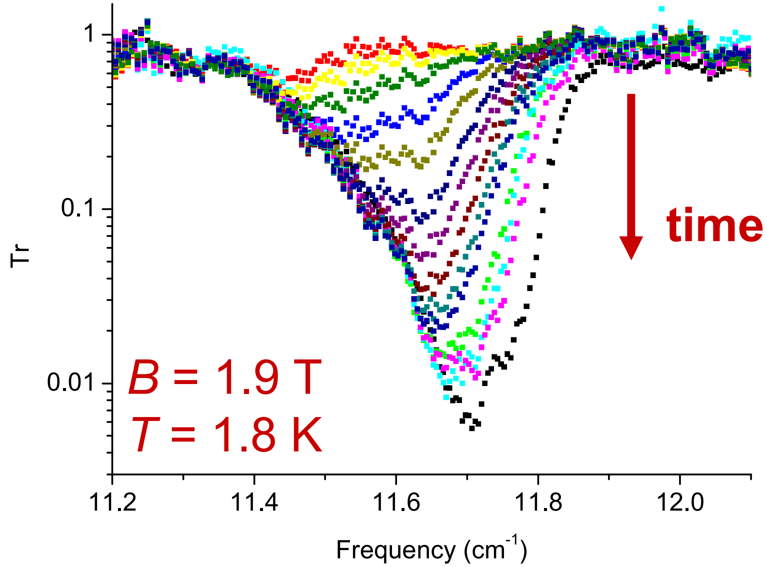

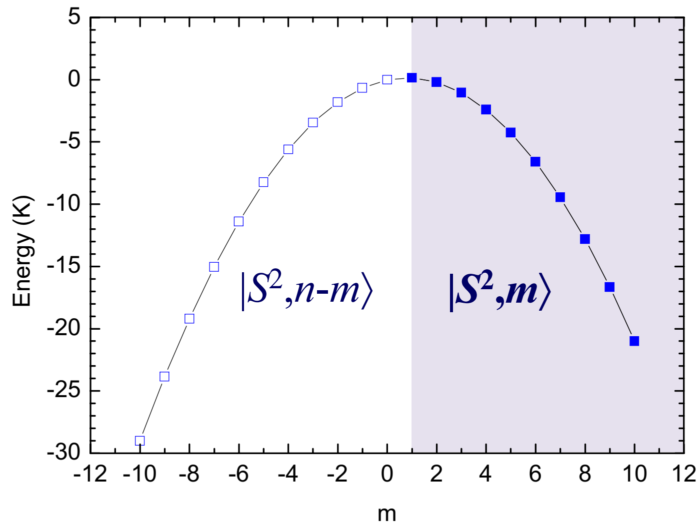

Magnetic Quantum Tunneling

spectroscopic investigations

- Increasing the magnetic field, we observe various **level crossings**.

Two minima in the relaxation time corresponding to level crossings: $m_S = -10$, 7 and $m_S = -10$, 6 respectively.

Inhomogeneous relaxation
Non-single-exponential relaxation curves

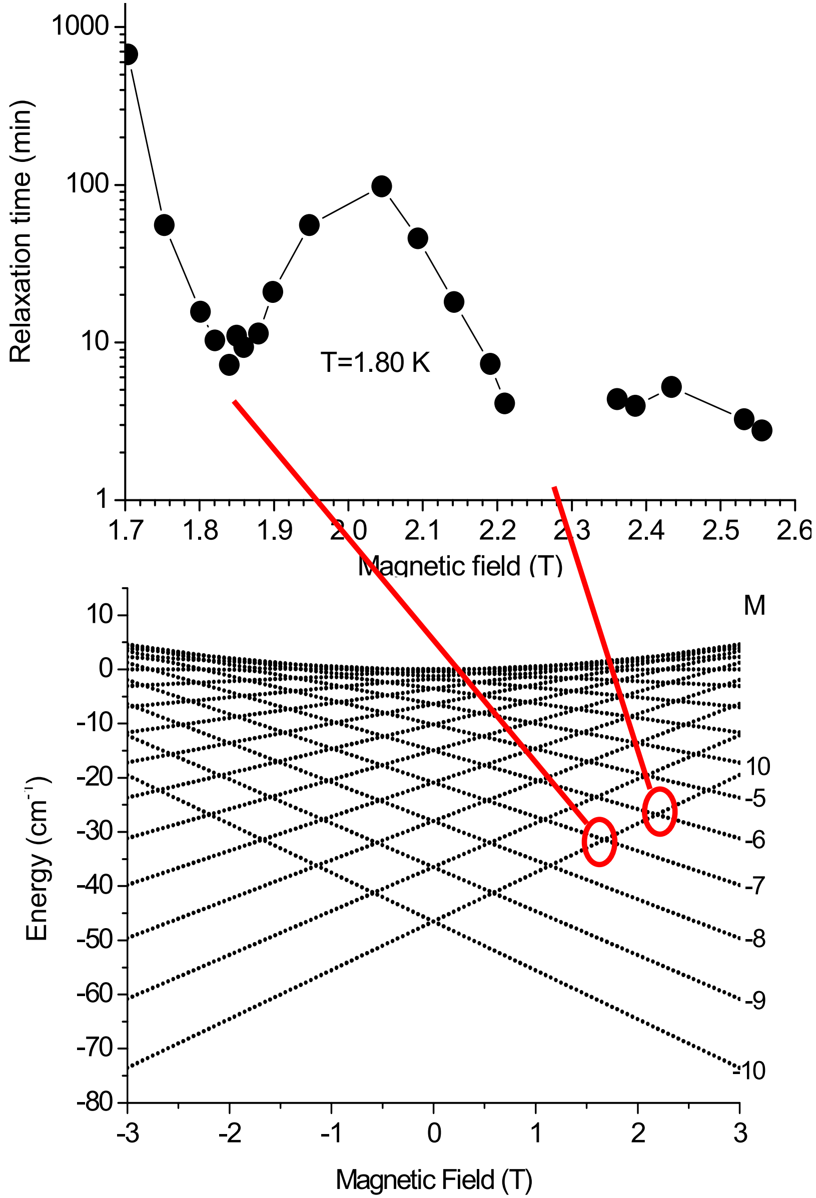

Magnetic Quantum Tunneling
spectroscopic investigations

- **Transverse field** increase with misalignment

The alignment is critical:
a deviation of 2 degrees gives a
threefold decrease in relaxation time.

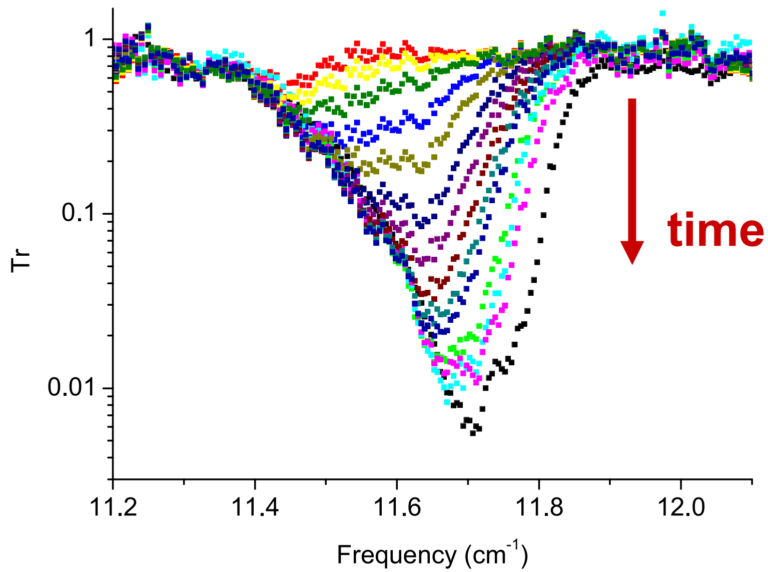

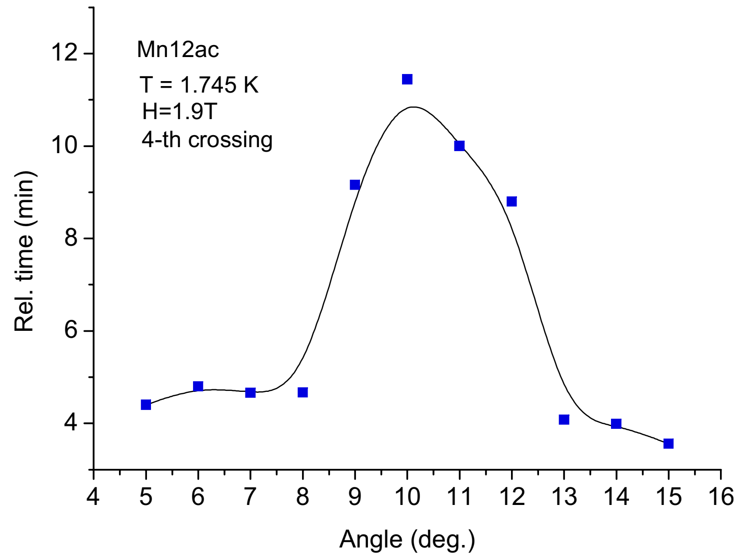

S. Vongtragool et al. 2003

Summary

frequency domain magnetic resonance spectroscopy on Mn_{12}ac

Using a new high-frequency ESR spectroscopy we are able to

- determine the parameters of the spin Hamiltonian;
- study of the energy levels, crystal field splitting,
  exchange and hyperfine interaction, influence of environment;
- study the magnetic bistability;
- study relaxation phenomena: thermal tunneling, quantum tunneling.

A.A. Mukhin, B. Gorshunov, M. Dressel, C. Sangregorio, D. Gatteschi
Phys. Rev. B **63**, 214411 (2001)

M. Dressel, B. Gorshunov, K. Rajagopal, S. Vongtragool, A.A. Mukhin
Phys. Rev. B **67**, 060405(R) (2003)

S. Vongtragool, B. Gorshunov, A.A. Mukhin, J. van Slageren, M. Dressel, A. Müller
Phys. Chem. Chem. Phys. **5**, 2778 (2003)

J. van Slageren, S. Vongtragool, B. Gorshunov, A.A. Mukhin, N. Karl, J. Krzystek, J. Telser, A. Müller, C. Sangregorio, D. Gatteschi, M. Dressel
Phys. Chem. Chem. Phys. 5, 3837 (2003)

S. Vongtragool, B. Gorshunov, M. Dressel, J. Krzystek, D.M. Eichhorn, J. Telser
Inorganic Chemistry **42**, 1788 (2003)

S. Vongtragool, A. Mukhin, B. Gorshunov, M. Dressel
Phys. Rev. B **69**, 104410 (2004)

J. van Slageren, S. Vongtragool, B. Gorshunov, A.A. Mukhin, M. Dressel
J. Magn. Magn. Mat. **272-276**, E765 (2004)

S. Vongtragool, B. Gorshunov, J. van Slageren, M. Dressel, A.A. Mukhin
J. Magn. Magn. Mat. **272-276**, E769 (2004)

J. van Slageren, S. Vongtragool, A. Mukhin, B. Gorshunov, M. Dressel
Phys. Rev. B **71**, (2005)